Single cell analysis

Wim De Malsche, Séverine Le Gac

Rationale

- Individual cell behavior ↔ collective behavior
- Specific for each cell (heterogeneity), time information ↔ population information
  - Analysis of rare cells
    - CTCs: few copies in 10 ml
    - Stem cells: fate of individual cells?
  - Analysis of heterogeneous samples (tissue, tumor)

- Identification (e.g. single cell treatment) → track and reuse cell of interest
- Molecules of interest: DNA, RNA, proteins, metabolites

Rationale

- Understanding the cellular response to therapeutics
- Study single cell response to stimuli, stress and environmental factors
- Understanding tumor heterogeneity and how this affects therapeutic resistance.
- Study proteome dynamics during biological transitions

Role of microfluidics in SSA

- Providing µstructures with dimensions compatible to cells
  - Structures 1-100 µm, porous walls sub-µm pores, cells µm range up to 30 µm
- Isolate individual cells (or arrays)
- Volumes and liquids in the nl range (and below)
  - Cell confinement
  - Minimize cell dilution in case of lysis (cell in pL range, 0.2 µl handling range for pipette)
- High control of (laminar) flow
  - Spatial and temporal control at the microscale

Laminar flow – addressing specific cell regions

Bovine capillary endothelial cell

Mitotracker Red CM-H2XRos

Mitotracker Green FM

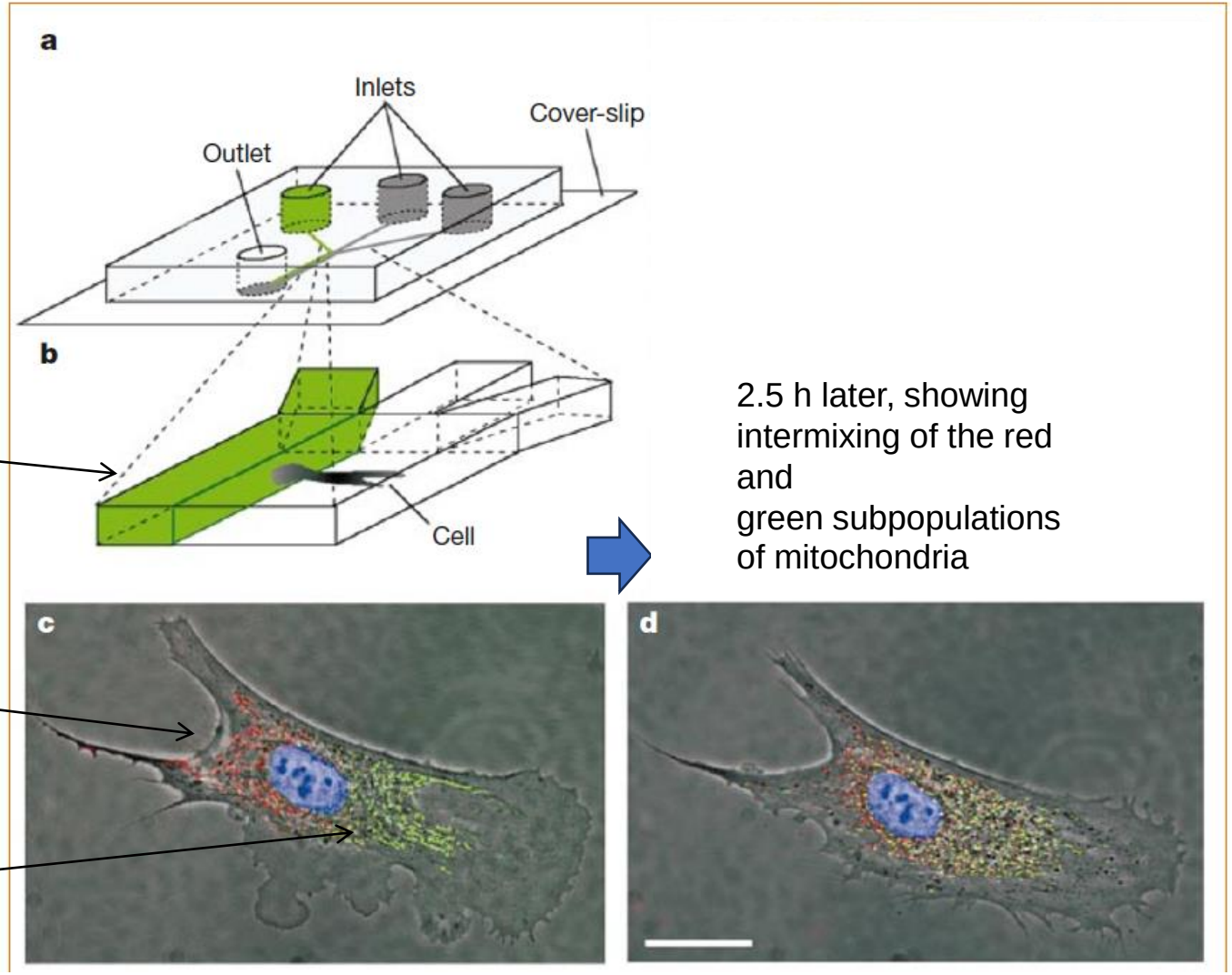

2.5 h later, showing intermixing of the red and green subpopulations of mitochondria

NATURE | VOL 411 | 28 JUNE 2001 | www.nature.com (Takayama et al)

Chemical analysis

Fluorescence detection of extracellular lactate by an optical fiber-based nanobiosensor

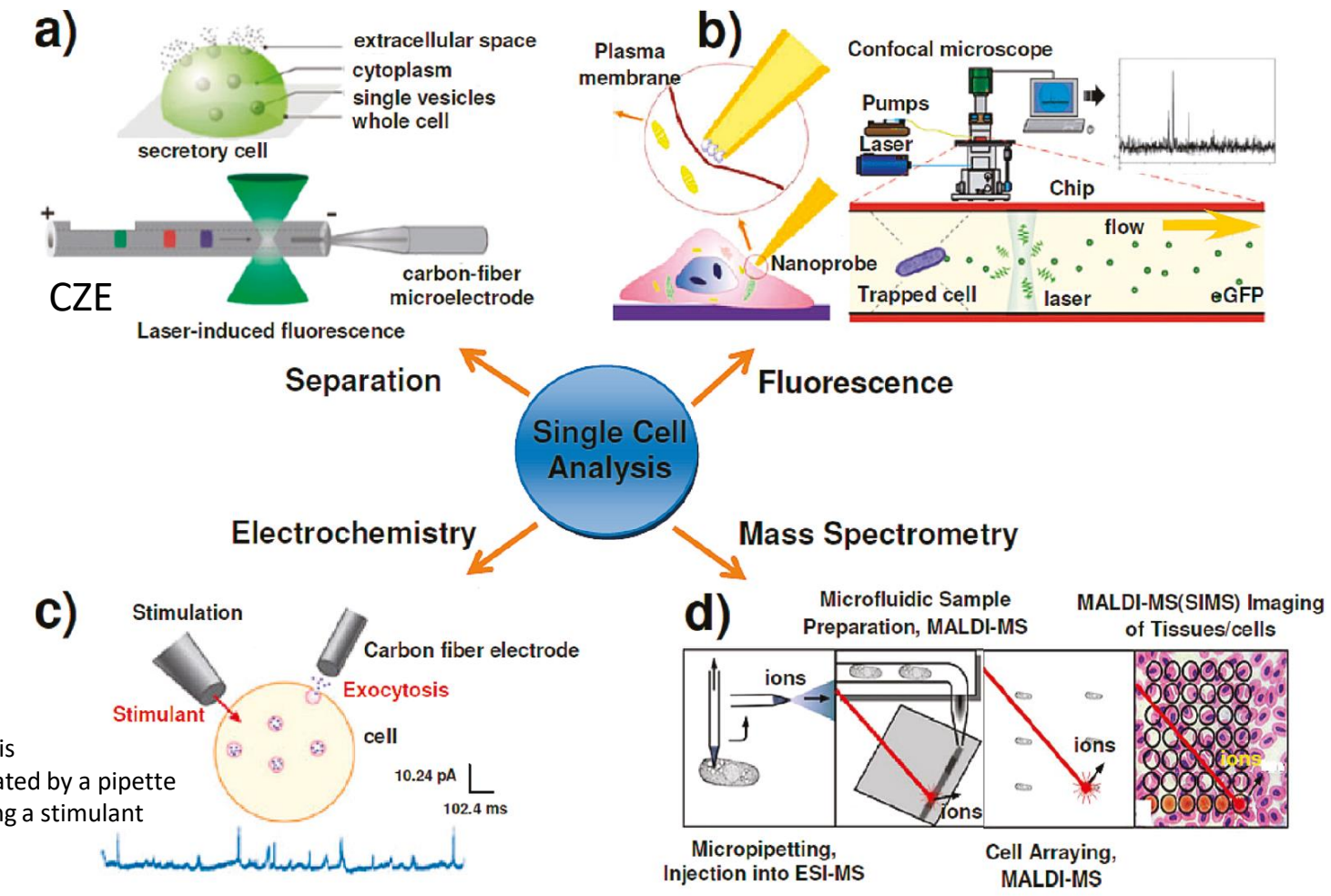

exocytosis
is stimulated by a pipette
containing a stimulant

Anal. Chem. 2011, 83, 4369–4392

Some history (CZE as separation method)

J. P. Martin, a pioneer in the field of chemical separations, said in 1962:
"The appetite of the chemist to work on a small scale will grow as it becomes more possible. He will be able to analyze and experiment on single cells. There is obviously an almost limitless field in making and using apparatus for measuring various physical properties on small objects."

Helix is a genus of large, air-breathing land snails native to the western Palaearctic and characterized by a globular shell (Wikipedia)

Science
AAAS

Microcolumn Separations and the Analysis of Single Cells

Author(s): Robert T. Kennedy, Mary D. Oates, Bruce R. Cooper, Beverly Nickerson and James W. Jorgenson

Source: *Science*, Oct. 6, 1989, New Series, Vol. 246, No. 4926 (Oct. 6, 1989), pp. 57-63

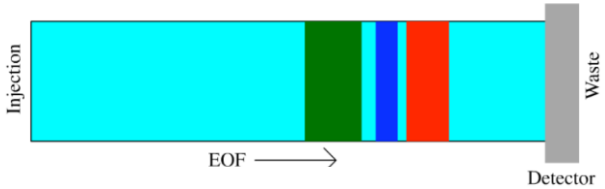

https://profiles.snsu.edu/cnm_tgc/primers/pdf/CEs.pdf

Helix neurons

The cell was removed from the ganglia by microdissection techniques and transferred to a microvial by means of a small pipette. The
The microvial consisted of a capillary that was melted closed at one end and could hold a total volume of 500 nl.

The cell was homogenized and centrifuged, and then the supernatant was removed and injected into an OTLC column (10 µm ID).
The detector for this work was a carbon-fiber microelectrode operated in the voltammetric mode

Amino acid profiling

The electrochemical detector that we have used is based on inserting a carbon-fiber microelectrode, which acts as the working or sensing electrode into the outlet end of the column. The electrode is cylindrical in shape and has a length of 0.1 to 1 mm and a diameter of 5 to 10 µm

Using this detector, we have obtained detection limits as low as 10^{-10} M, or 1 amol (10^{-18} mol), based on a 10 nl injection volume

Table 2. Amino acid profiles of individual neurons of *Helix aspersa*. The values for E4 are the mean ± standard deviation (n = 5); the values for D2 and F1 are the values obtained in a single analysis of each cell.

Peak (Fig. 3)	Amino acid	Measured amount in cell (fmol) (10^{-15} mol)		
		E4	D2	F1
1	Asp	500 ± 100	560	300
2	Glu	1,300 ± 440	6,000	430
3	Asn	300 ± 130	940	500
4	Ser	950 ± 370	2,300	570
5	Gln	1,900 ± 1,100	14,000	930
6	His	320 ± 55	1,000	110
7	Gly	870 ± 300	2,400	510
8	Thr	290 ± 24	920	140
9	Ala	4,200 ± 2,400	25,000	2,100
10	Arg	39 ± 14	56	73
11	Tyr	260 ± 100	500	80
12	Val	200 ± 63	950	150
13	Met	120 ± 57	210	48
14	Trp	69 ± 28	130	19
15	Ile	170 ± 46	860	110
16	Phe	380 ± 160	1,300	290
17	Leu	250 ± 150	870	160

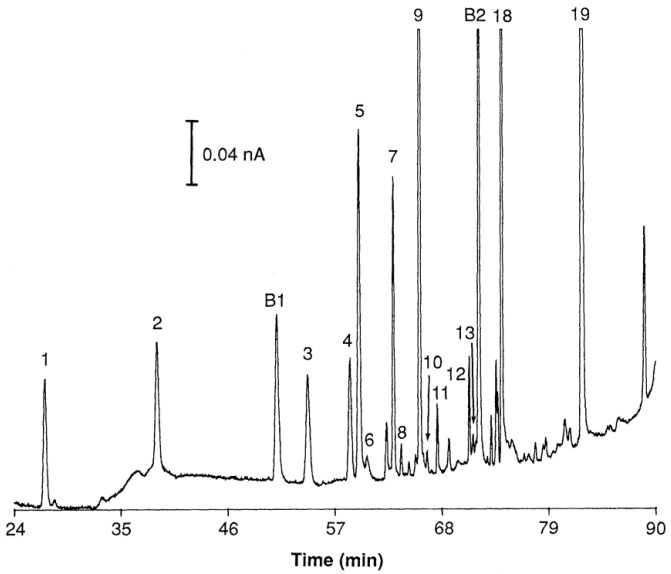

Fig. 3. Chromatogram of NDA-tagged amino acids from cell F1. Peak numbers 1 to 17 correspond to those listed in Table 2. Peaks 14 to 17 appear between B2 and peak 18. B1 and B2 are present in blanks, and peaks 18 and 19 are the internal standards norleucine and normetanephrine, respectively. All unlabeled peaks are unknowns found in the cell. Mobile phase A was 3% tetrahydrofuran in 0.05*M*, *p*H 7.0, sodium phosphate buffer; mobile phase B was acetonitrile. A linear gradient was used as follows: 100 to 89% A and 11% B in 38 min, and then to 47% A and 53% B in 80 min.

Dimensions and protein content cells

Table 1 Dimensions and protein content of common cell types used in biomedical research

Cell type	Cell diameter	Cell volume			protein quantity		
	(µm)[a]	µm^3 or fL	pL	nL	µg	ng	pg
Xenopus oocyte	999	1.0E+09	1.0E+06	1.0E+03	2.0E+02	2.0E+05	2.0E+08
megakaryocyte	31.1	30000	30.0	3.0E-02	6.0E-03	6.0000	6000
osteoblast	15.9	4000	4.0	4.0E-03	8.0E-04	0.8000	800
HeLa, MDCK, Jurkat, K562, HEK293, fibroblast, beta cell	14.4	3000	3.0	3.0E-03	6.0E-04	0.6000	600
	12.6	2000	2.0	2.0E-03	4.0E-04	0.4000	400
MDCK cell	7.9	500	0.5	5.0E-04	1.0E-04	0.1000	100
neutrophil	6.7	300	0.3	3.0E-04	6.0E-05	0.0600	60
red blood cell	4.6	100	0.1	1.0E-04	2.0E-05	0.0200	20
yeast	3.3	35	0.035	3.5E-05	7.0E-06	0.0070	7
Ecoli	0.9	0.8	0.001	8.0E-07	1.6E-07	0.0002	0.2

[a]Xenopus oocyte diameter range 1.0-1.3 mm [31]. The red blood cell has a discoid shape of diameter ~8.0 µm, thickness of 2.2 µm and volume ~100 µm^3 [32]. All other cell volumes based on Cell Biology by the Numbers [33]. Cellular protein concentration assumed 200 g/L [34]

Analytical and Bioanalytical Chemistry (2024) 416:2359–2369

Examples single cell protein analysis (MS)

Table 1
Overview of selected papers related to single cells/related samples.

Cell types	Cell number/ protein amount	Number of proteins/ protein groups	Sample preparation	Column format ID (μm) x length (cm)	Stationary phase	Flow rate in nL/min (gradient time)	Trap column	Emitter	Mass spectro-meter	Ref.
HeLa cells (also single human pancreatic islets)	12 cells	Ca. 3200*	NanoPOTS[a]	30 × 70 (Pico-frit)	3 μm 300 Å C18 particles	60 (150 min)	100 μm × 4 cm packed with 3 μm 300 Å C18 particles	10 μm ID integrated	Orbitrap Fusion Lumos Tribrid	[8]
Mouse embryonic stem cells (Also Jurkat and U937 cells)	Single	>1000**	SCoPE[b]	75 × 20	1.8 μm 200 Å C18 particles	200 (170 min)	150 μm × 5 cm packed with 5 μm 100 Å C18 particles	20 μm ID, 15 μm pico-tips	LTQ Orbitrap Elite	[9]
HeLa	Single	Ca. 870*	NanoPOTS[a]	20 × 60	3 μm 300 Å C18 particles	20 (100 min)	75 μm × 5 cm packed with 3 μm 300 Å C18 particles	10 μm ID in-house etched	Orbitrap Eclipse Tribrid	[21]
Shewanella oneidensis	75 pg tryptic peptides	Ca. 1000*	Solid phase extraction	2 × 80	A layer of C18	0.79 (30 min)	Not used	In-house etched on column (2 μm)	Orbitrap Fusion Lumos Tribrid	[33]
Myeloid leukemia cells (Also HeLa cells)	Ca. 10	251 ***	Solid phase extraction	20 × 35	Poly(styrene-co-divinylbenzene) monolith	12 (60 min)	Not used – Loading for 60 min at 50 nL/min)	10 μm × 3 cm distal coated	FAIMS[d] - Orbitrap Fusion Lumos Tribrid	[14]
Monocytes and macrophages	Single	Ca. 1000**	SCoPE2[e] features mPOP[f]	75 × 25	1.8 μm C18 particles	200 (53 min)	Not used- loading for 20 min	Integrated on column	Q-Exactive Orbitrap	[10]
HeLa (Also single motor neurons and interneurons from human spinal tissue)	Single	Ca. 1050***/ 683**/ 1475*	nanoPOTS[a]	20 × 50	3 μm 300 Å C18 particles	20 (100 min)	Off-line: 75 μm ID packed with 3 μm 300 Å C18 particles	Not described	FAIMS[d] - Orbitrap Eclipse Tribrid	[15]
HeLa	Single	Ca. 840*	EvoSep	75 × 15	1.9 μm C18	100 (35 min)	EvoTips	10 μm ID	TimsTOF[g] Pro	[26]
HeLa	250 pg tryptic peptides	1486***	Dilution	157 × 3 (width x height)	μPAC Gen2 nonporous silicon pillars	250 (60 min)	Not used	10 μm ID	FAIMS[d] – Orbitrap Exploris™ 480	[43]

250 pg peptides ~ content single cell

[a]nanoPOTS: nanodroplet Processing in One pot for Trace Samples; [b]SCoPE: Single Cell ProtEomics; [c]TMT: tandem mass tag, [d]FAIMS: high-field asymmetric waveform ion mobility spectrometry; [e] SCoPE2: Single Cell ProtEomics version 2; [f]mPOP: Minimal ProteOmic sample Preparation; [g]TimsTOF: trapped ion mobility mass spectrometry time of flight; * Searches performed with match between runs algorithm in MaxQuant. ** Searches performed with MaxQuant.*** Searches performed with Proteome Discoverer.

Analytica Chimica Acta 1178 (2021) 338551

Pillar array columns – some molecule types

5 µm diameter, 2.5 µm spacing

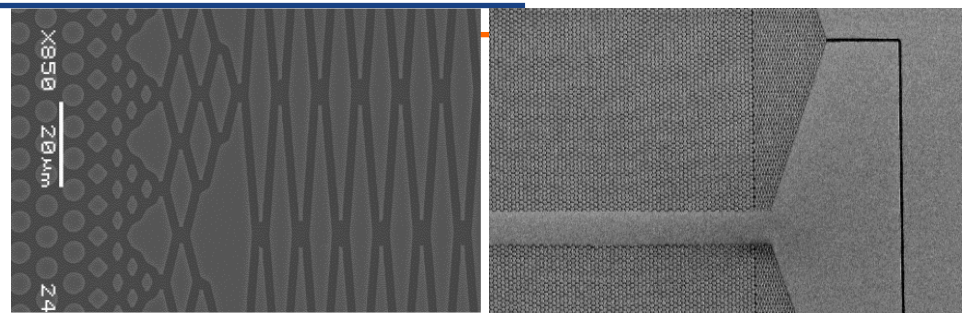

Flow distribution for plug conservation in inlets and turns

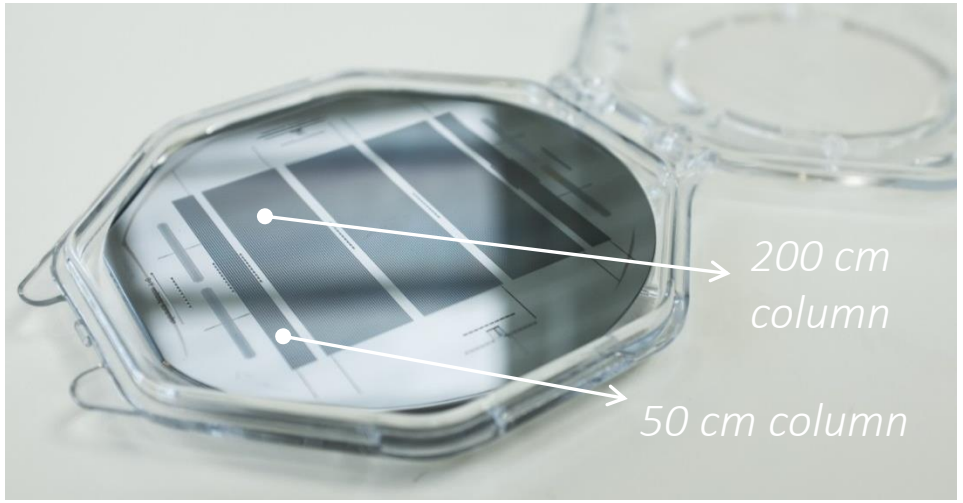

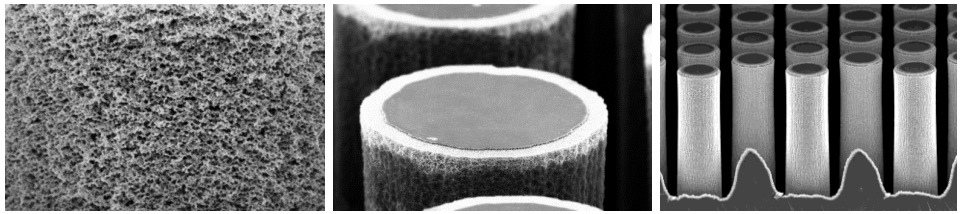

Backbone of the stationary phase: porous Si (anodization) or SiO_2 (sol-gel)

Hela cell digest, limited sample

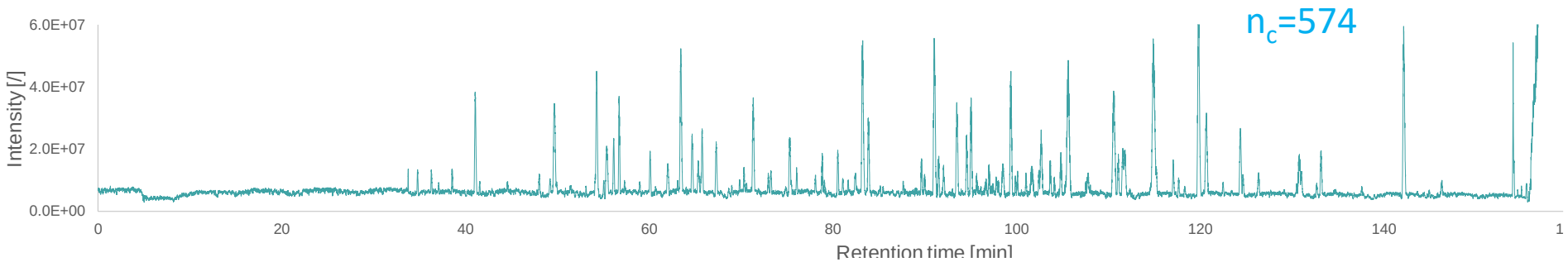

10 ng HeLa cell digest ≈

protein content of ± 50 cells

- Over 15.000 unique peptide ID's in 120 min
- Over 3.000 protein ID's in 120 min

Experimental conditions

10 ng HeLa cell digest – 1 µl injection
2 to 40% ACN / 0.1% FA
120 min gradient / 300 nl/min

system: Thermo Scientific EasynLC 1200
Detection: Thermo Scientific Orbitrap Fusion™ Lumos™ Tribrid™ mass spectrometer

HeLa is an immortalized cell line used in scientific research. It is the oldest human cell line and one of the most commonly used. HeLa cells are durable and prolific, allowing for extensive applications in scientific study. The line is derived from cervical cancer cells taken on 8 February 1951, from Henrietta Lacks, a 31-year-old African American mother of five, after whom the line is named. Lacks died of cancer on 4 October 1951. (Wikipedia)

µPAC™-MS Lipidomics Platform

Separation of human blood plasma lipid extract

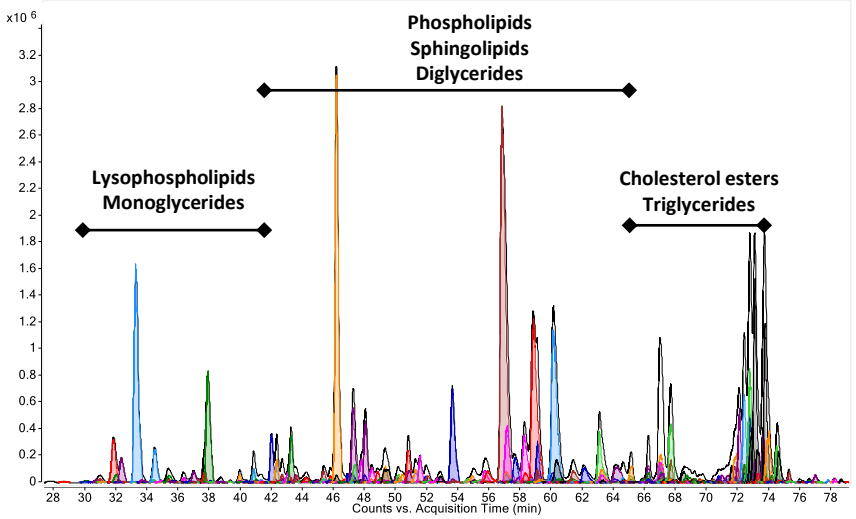

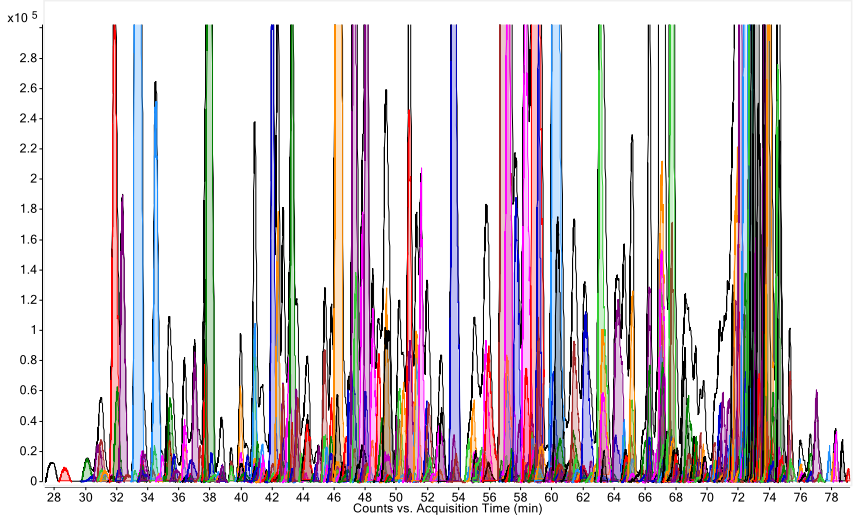

Enormous sample complexity is revealed

INTER-class lipid separation

- All major lipid classes are detected

INTRA-class lipid separation

- Number of carbons
- Degree of saturation in fatty acid side chains
- Fatty acid side chain position & composition

Experimental conditions

Lipid extract from 100 µl EDTA blood plasma – 50 nl injection
30 to 98% B in 60 min – 750 nl/min
A: 20mM NH_4HCO_2 (PH 5)
B: C_3H_7OH/CH_3OH (90/10) (v/v)

RIC Research Institute for Chromatography

µPAC™-MS Lipidomics Platform

Inter-class separation of ceramide glycosphingolipids

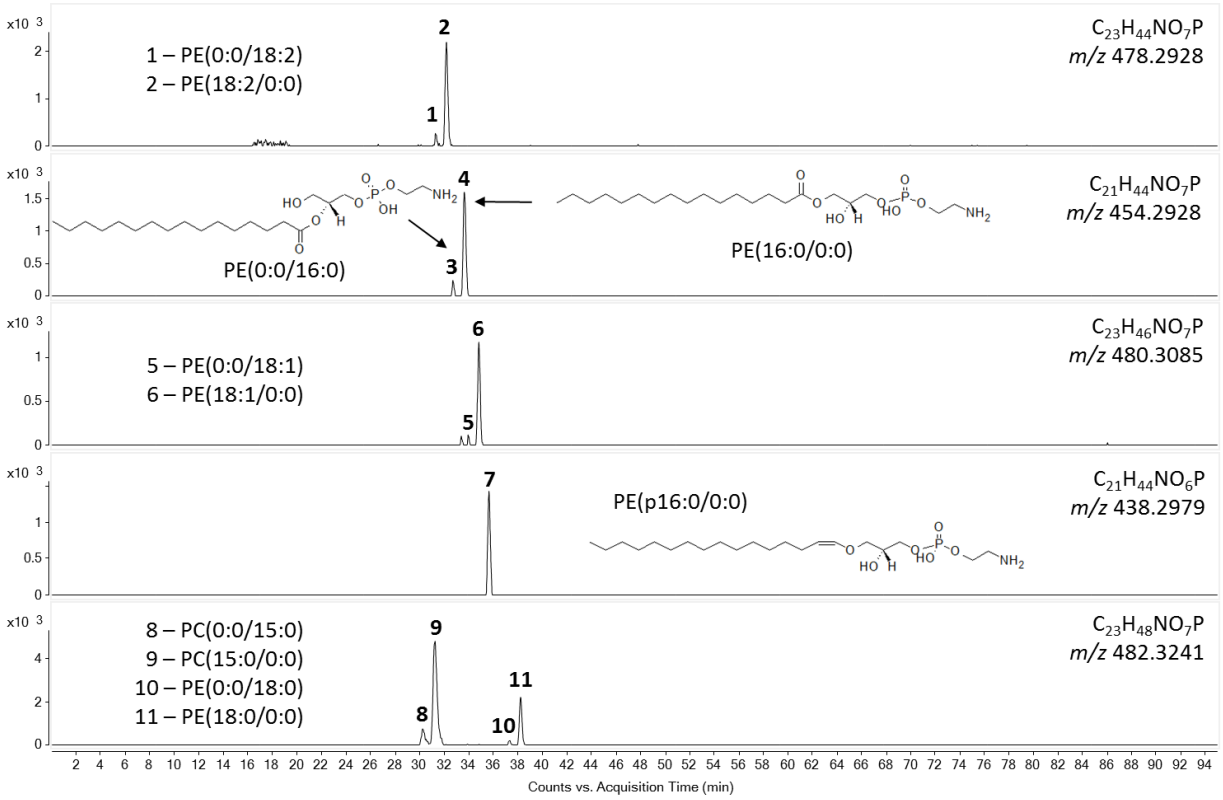

Separation by:

→ Number of carbon atoms

- Lyso-PE (16:0) → peaks 3 & 4
- Lyso-PE (18:0) → peaks 10 & 11

→ Degree of saturation

- Lyso-PE (18:2) (2 C=C bonds) → peaks 1 & 2
- Lyso-PE (18:1) (1 C=C bond) → peaks 5 & 6
- Lyso-PE (18:0) (no C=C bonds)→ peaks 10 & 11

→ Fatty acid chain position

- Lyso-PE (0:0/16:0) (*sn*-2 position) → peak 3
- Lyso-PE (16:0/0:0) (*sn*-1 position) → peak 4

→ Fatty acid composition

- Lyso-PC (15:0) → peaks 8 & 9
- Lyso-PE (18:0) → peaks 10 & 11

RIC Research Institute for Chromatography

µPAC™-MS Metabolomics Platform

Plant Metabolomics

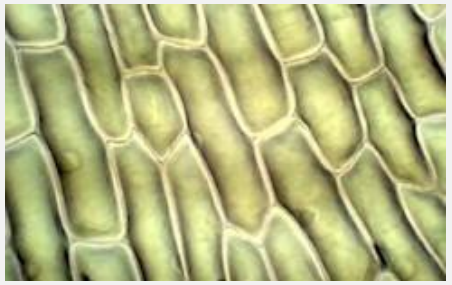

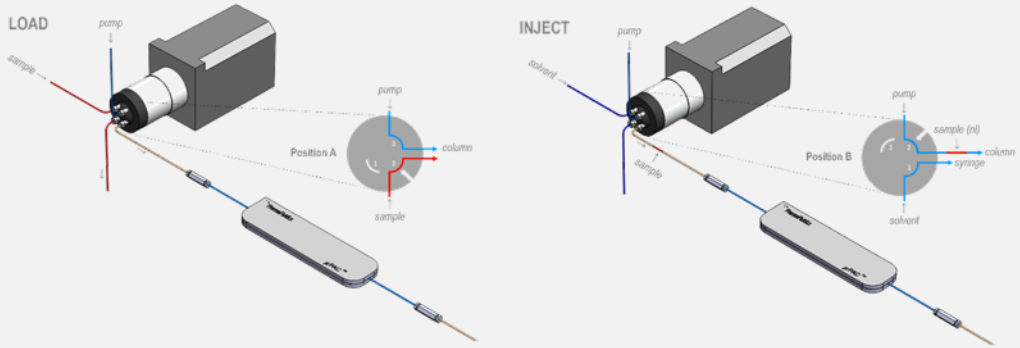

Increased intensity for a factor 1,250 less sample load

1260 Infinity Nanoflow LC
Nano ESI (Advion coupler)
LTQFT

Accela
ESI
LTQFT

Poplar bark metabolite extract

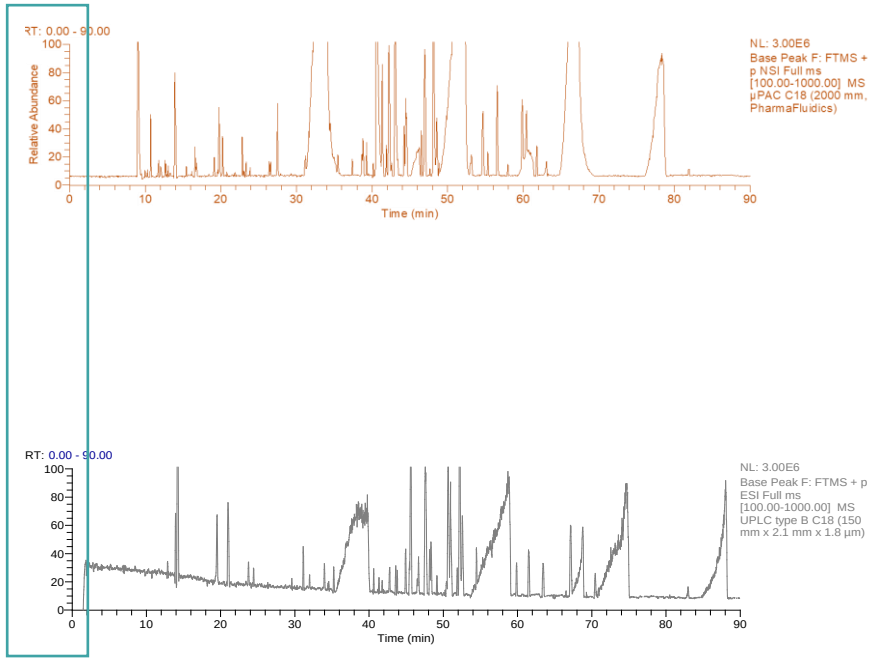

µPAC™ 200 cm; C18
Poplar bark metabolite extract – 4 nl injection
1 to 50% B in 120 min – 1 µl/min

Ref B: C18 (15 cm x 2.1 mm; 1.8 µm particles)
Poplar bark metabolite extract – 5 µl injection
1 to 50% B in 120 min – 300 µl/min

A: H_2O (100%) with 0,1% FA; B: C_2H_3N/H_2O (80/20) with 0,1% FA

VIB

Plant Systems Biology
A VIB-UGENT DEPARTMENT

Typical single cell experiments

Single cell technologies, '21

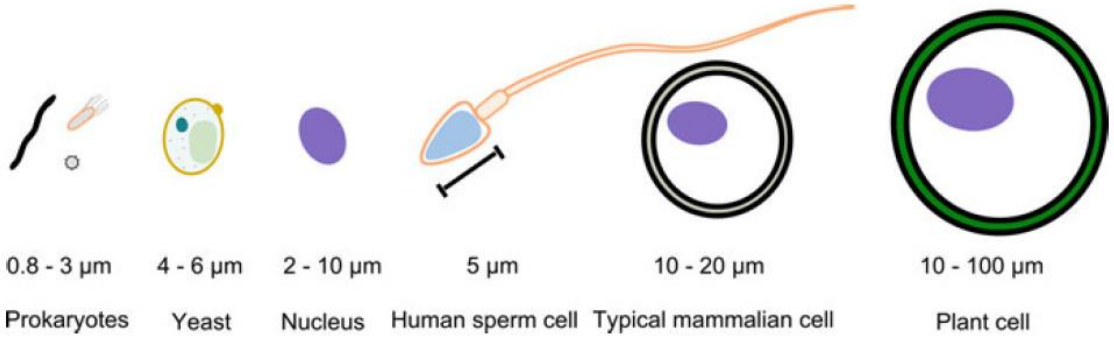

Fig. 2 Illustration of common cell types and their typical shapes and size ranges in suspension

- Analysis
  - Collection and analysis of specific molecules (DNA, RNA, proteins,…)
- Treatment
  - Exposure to chemical stimuli (followed by analysis)
- Cell engineering
  - Cell electroporation, intracellular injection, cell fusion

Cell trapping and manipulation tools critical for all activities

Single cell manipulation

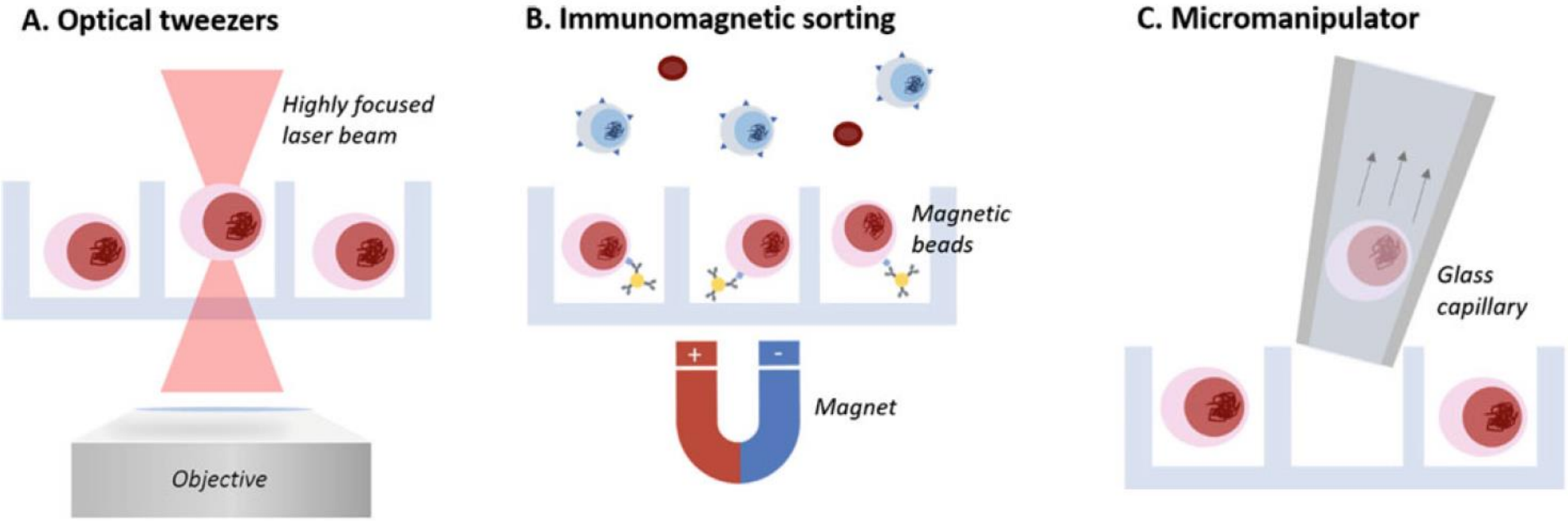

Single cell technologies, '21

Lysis - time and volume considerations

Fast lysis process:

- Snapshot on the cell content at a given time point (faster than biological processes (~ms timescale)

Avoid dilution of the retrieved biological material

- Cell: 1 pL, Microchamber (50 µm diam.; 20 µm height): 0.15 nL
- ⇨ 150 x dilution!!!!
- ⇨ Need for confinement of the lysate

No degradation of the biomolecules to be analyzed should occur

Specific to the cell plasma membrane

- Organelles (e.g., nucleus) kept intact

Cell lysis

- Gain access to cellular content
- Rupture of phospholid assembly
- Chemical lysis
- Electrical lysis
- Optical lysis
- Mechanical lysis

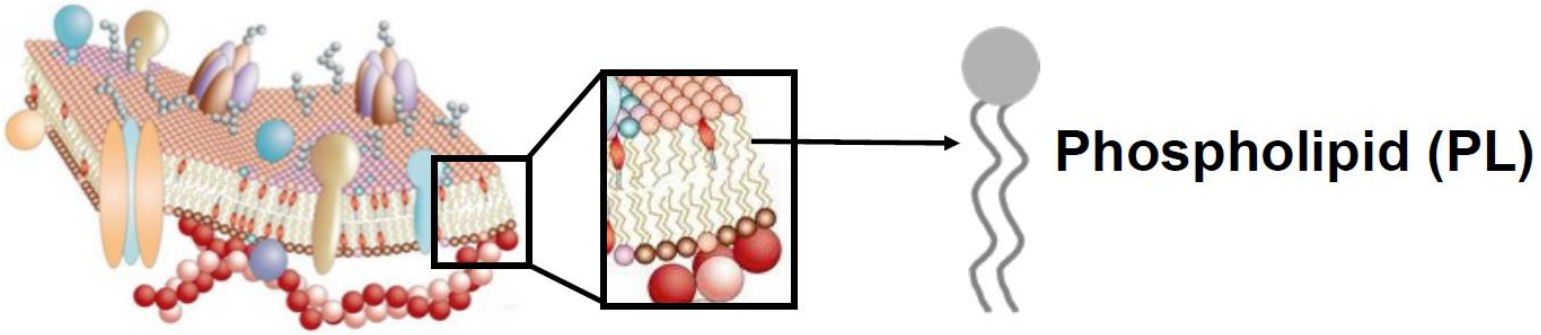

Single cell technologies, '21

Cell Lysis

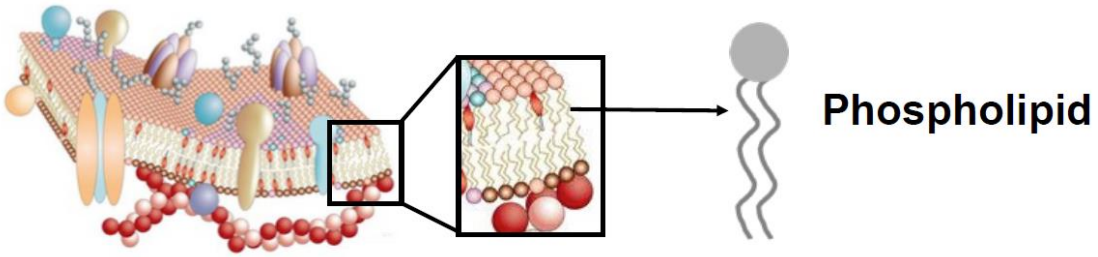

Techniques	How?	Principle	Timescale	Issues Advantages
Chemical lysis	Detergents	PL dissolution	Sec.-min.	- Mixing of the lysis and cell solutions - Δt lysis >> Δt bio_processes - Biological loss by diffusion - Lysate contamination
	Alkaline conditions (OH-)	PL hydrolysis	100 millisec. - sec.	
Electrical lysis	HV pulses	Irreversible membrane poration	Millisec.	- Need for (integrated) electrodes + Specificity for plasma membrane
Mechanical lysis	Nano-/sharp structures	Shear forces	Min.	- Addition of sharp structures - Slow process
"Optical" lysis	Laser pulse	Indirect heating?	Sub-millisec.	- Laser: $$$$$ - Need for optical expertise
Thermal lysis	ΔT℃ pulse	Dissociation of the PL assembly	Sec.-Min.	- Local heating? - Protein denaturation

Courtesy S. Le Gac

Toolbox: micro-and nanopore technologies

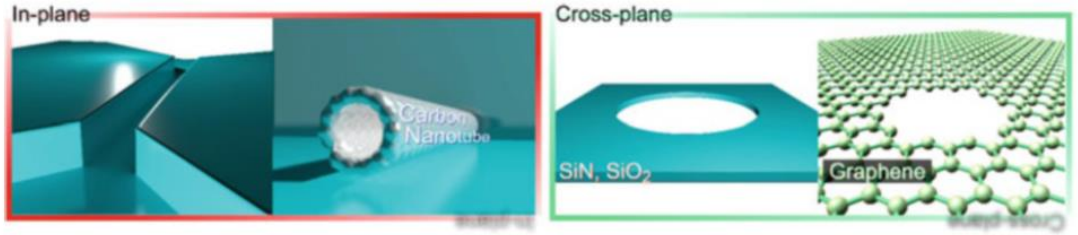

Type	Procedure		Pore size	Description
Cross-plane	Electron and ion beam milling	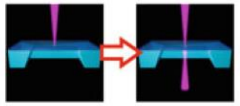	Sub nm ~ several 10 nm	Focused electron or ion beam is irradiated to penetrate a nanopore under a feedback control through measuring the cross-membrane current
	Dielectric breakdown	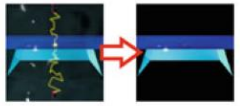	Sub nm ~ several 100 nm	Transmembrane voltage is controlled to cause dielectric breakdown of a thin dielectric membrane for forming a nanoscale conduit
	Glass nanopipette	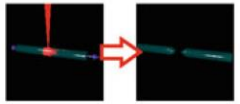	> 5 nm	Glass pipe is pulled to narrow the laser-heated portion via necking deformation down to nanometer scale
	Lithography	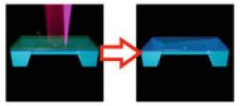	> 20 nm	A pore is delineated by an electron beam lithography and the residual resist is used as a mask for drilling a pore by dry etching
	Tunable nanopore	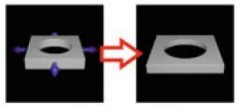	40 nm ~ 10 um	A pore of mechanically-adjustable diameter can be obtained by controlling the stretching deformation of an elastic membrane
	Material coating	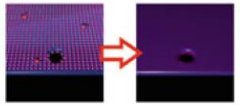	—	Metal and other materials can be deposited on membrane surface to finely tune the size of pore

In-plane	Focused ion beam lithography	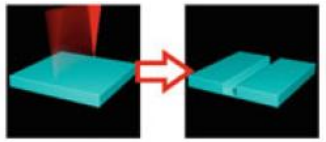	> sub 5 nm	Fluidic channels can be directly lithographed in a thin dielectrics by focused ion beam milling
	Electron beam lithography	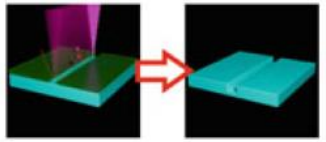	> 1 nm	Fluidic micro- and nanochannels can be created by direct electron beam lithography or with a post dry eching process
	Nanoimprint lithography	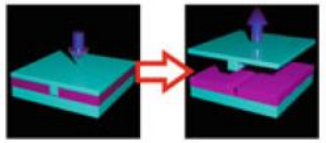	> 5 nm	A mold substrate is mechanically pressed on a soft material and subsequently removed that allows large-area formations of fluidic channel patterns
	Carbon nanotube	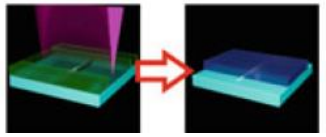	several nm	A thin dielectric layer is formed on a carbon nanotube by MEMS technique to use the hollow space as a nanochannel

Functions of solid micro-and nanopores

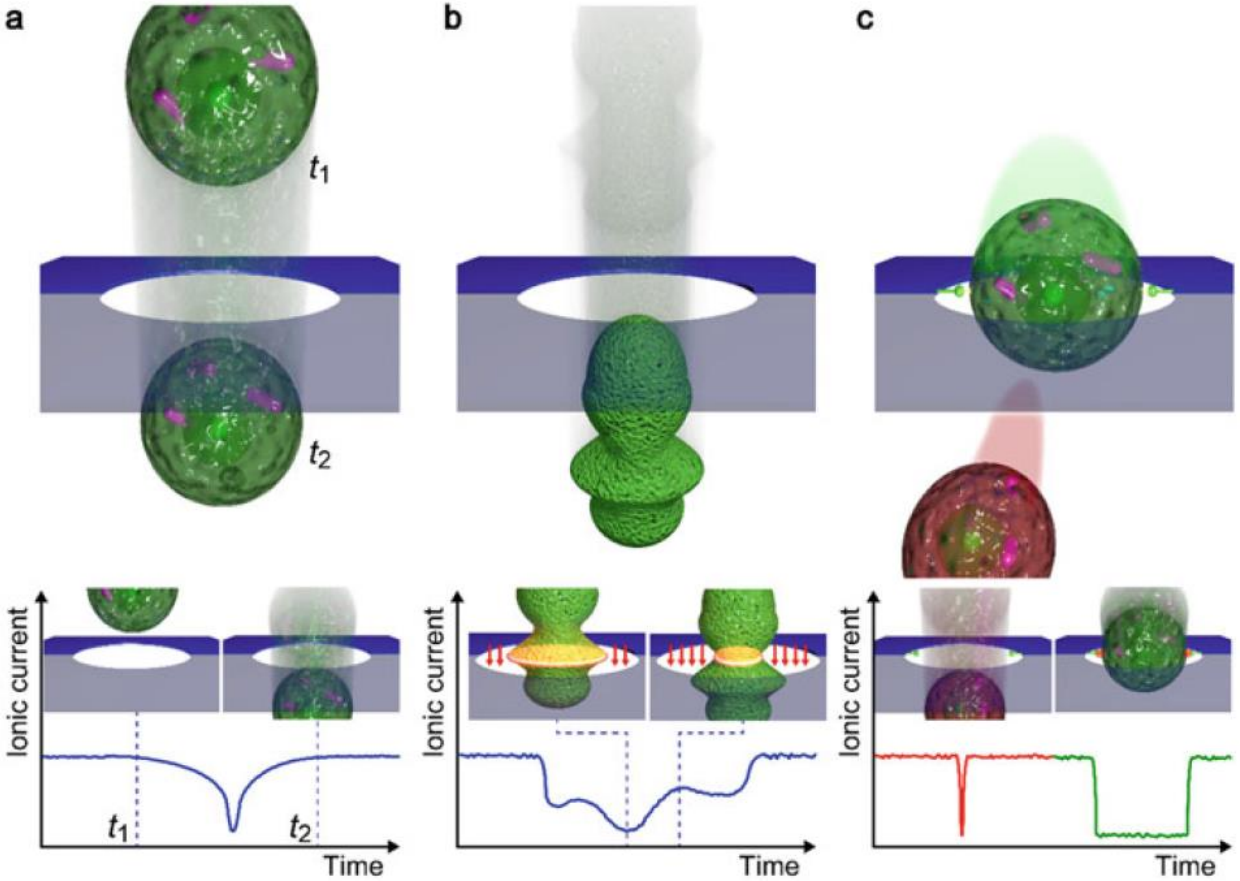

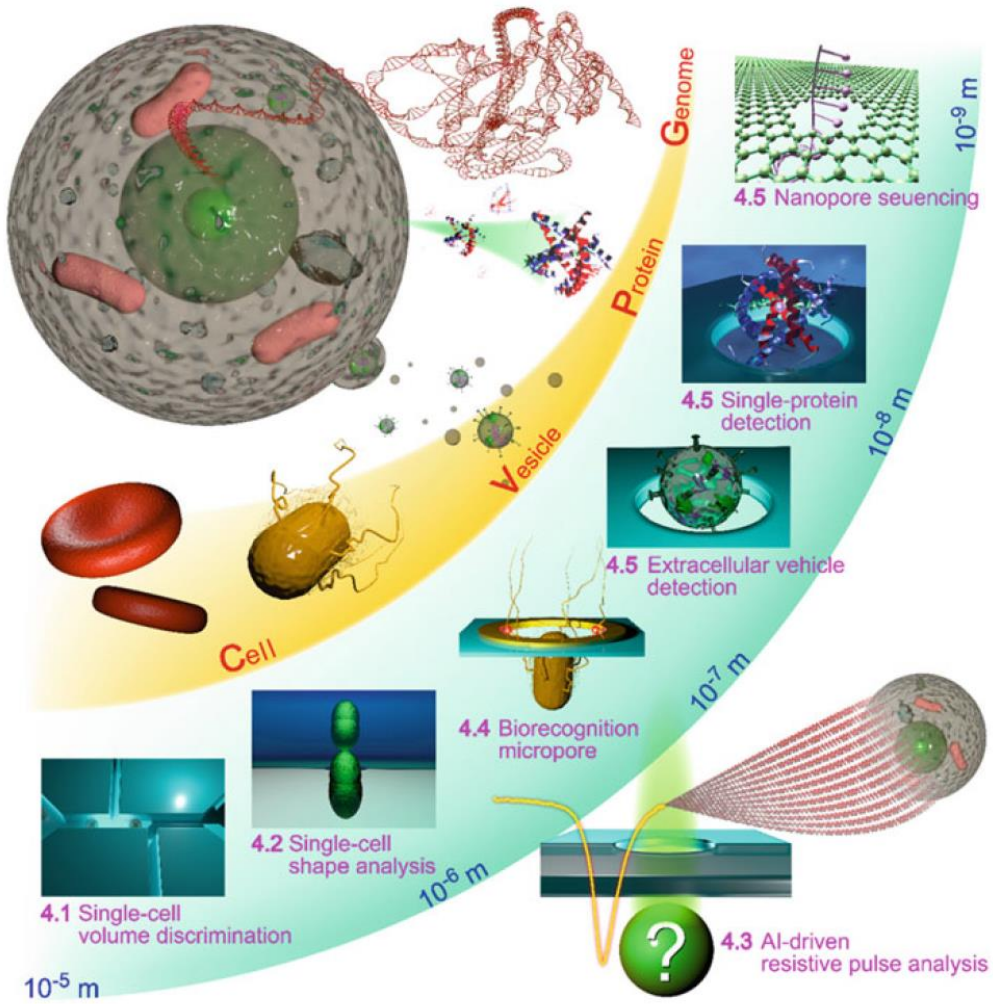

Single cell technologies, '21

Electroporation

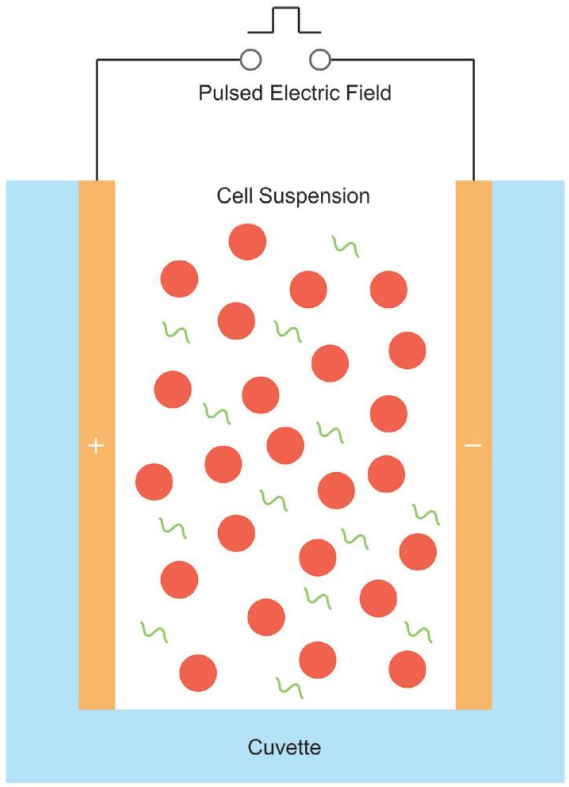

Fig. 1 Schematic of conventional bulk electroporation. The red circle represents a single cell, which is smaller than the distance between the electrodes by several orders of magnitude. The green curve represents the cargos to be loaded.

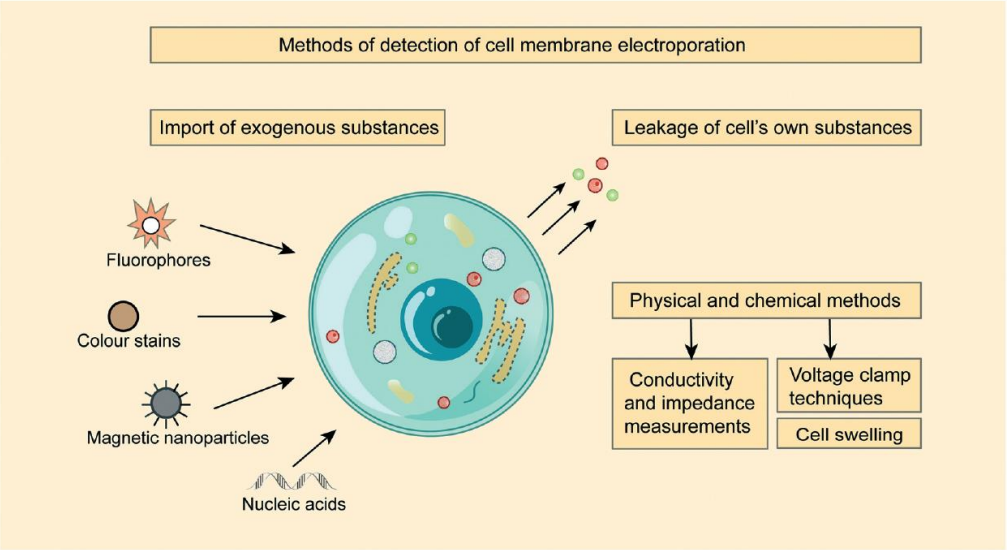

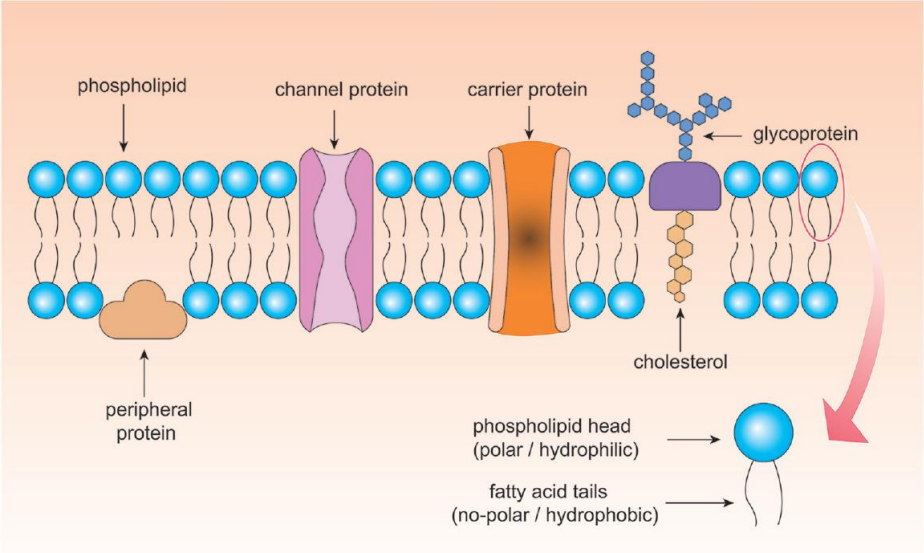

Lab Chip, 2022, 22, 2624–2646

Pore formation

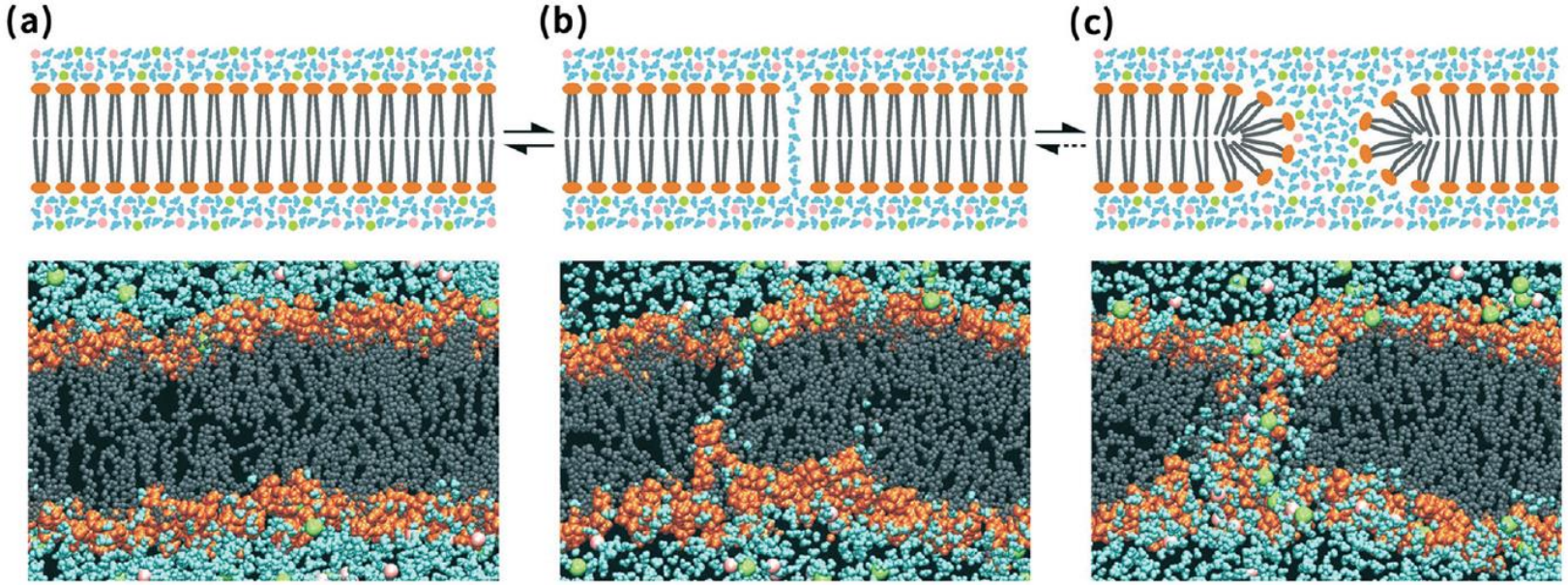

Fig. 3 Ideal dynamic simulation of electroporation at the molecular level (top) and atomic level (bottom) with the electric field perpendicular to the bilayer plane. (a) Intact bilayer. (b) Process of water molecules penetrating the bilayer. (c) Reorientation of lipids. Reprinted with permission from ref. 41. Copyright 2013, *J. Physics of Life Reviews*.

Wang et al, Lab Chip, 2022, 22, 2624–2646

Flow-through electroporation device

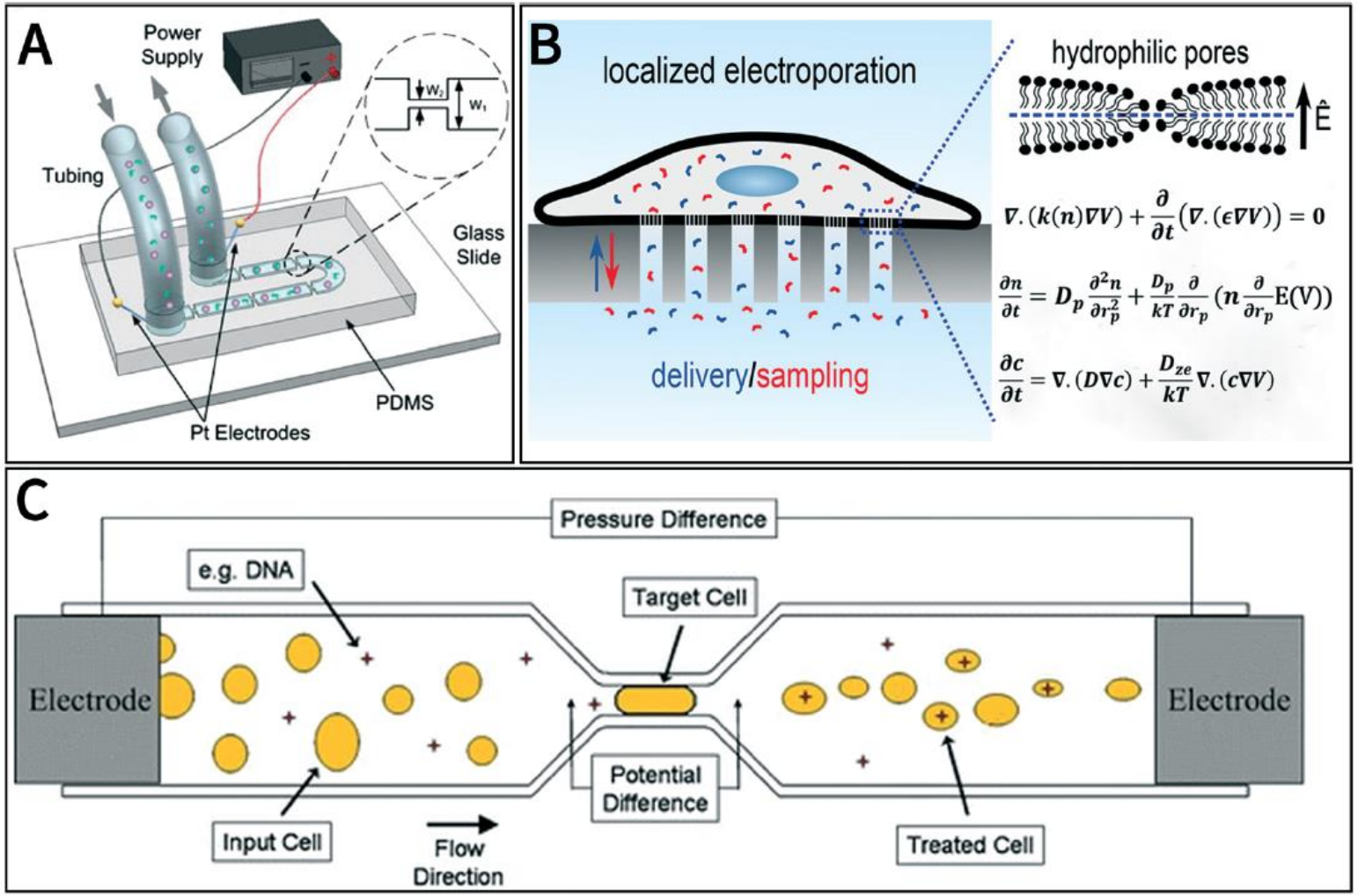

Wang et al, Lab Chip, 2022, 22, 2624–2646

Electroporation using micro/nanoelectrodes

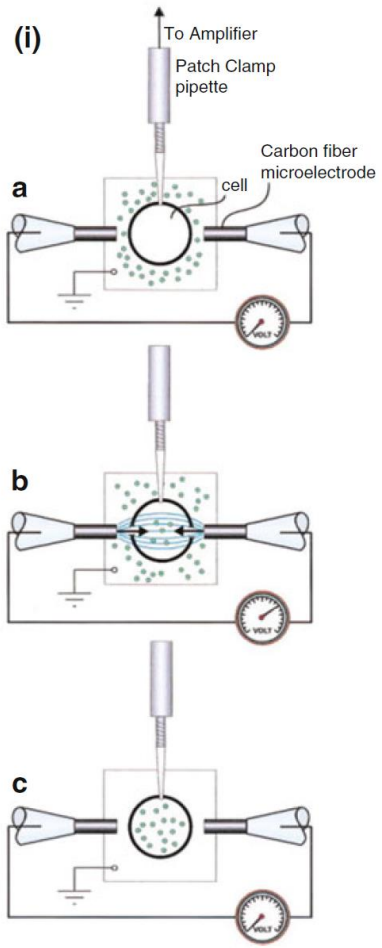

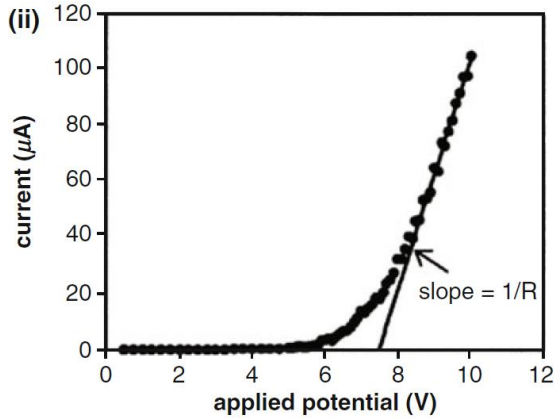

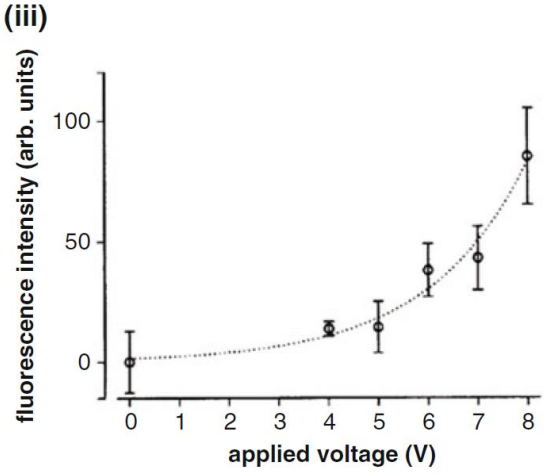

A patch-clamp pipette provides electrical current recording at each step of the voltage applied to the cell under test

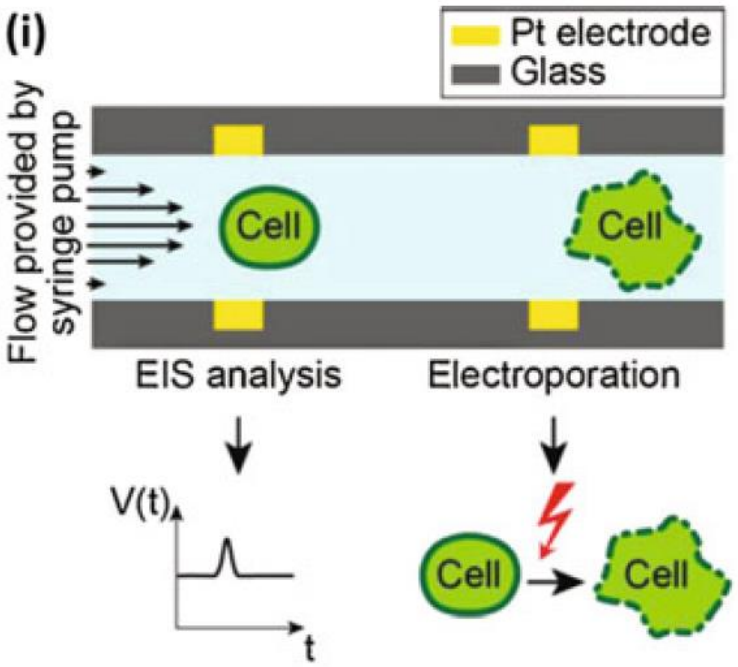

Single cell technologies, '21

Microelectrode configurations

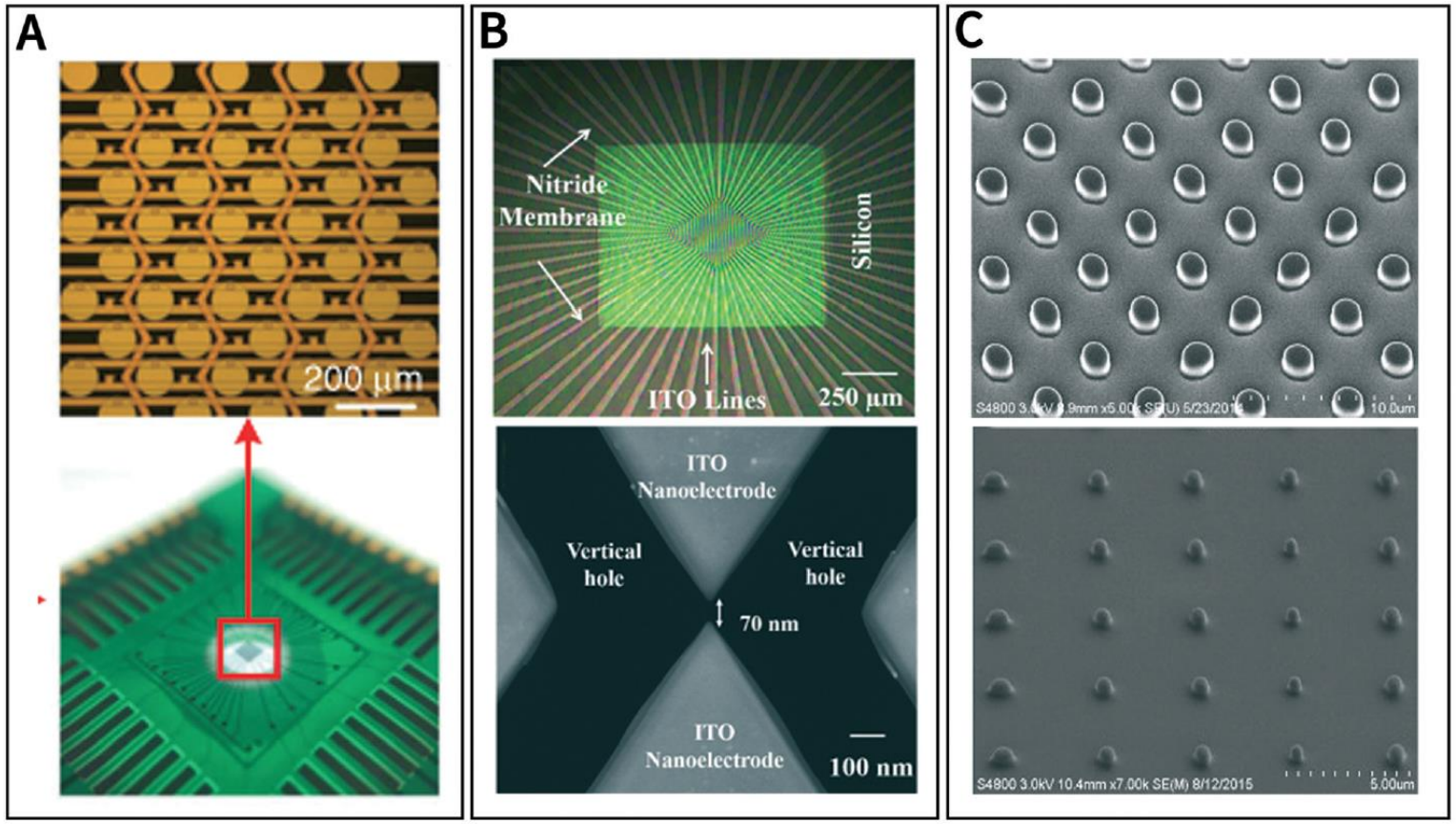

Fig. 6 (A) Schematic view of the microelectrode unit on the chip. Reprinted with permission from ref. 23. Copyright 2020, *Microsystems & Nanoengineering*. (B) SEM image of ITO nano-electrodes with 70 nm gaps. Reprinted with permission from ref. 20. Copyright 2020, *Lab on a Chip*. (C) SEM images of micropillar array made of SU-8 and carbon. Reprinted with permission from ref. 12. Copyright 2019, *Bioelectrochemistry*.

Wang et al, Lab Chip, 2022, 22, 2624–2646

Intracellular microinjection

Microinjection in cells using an integrated standard glass needle

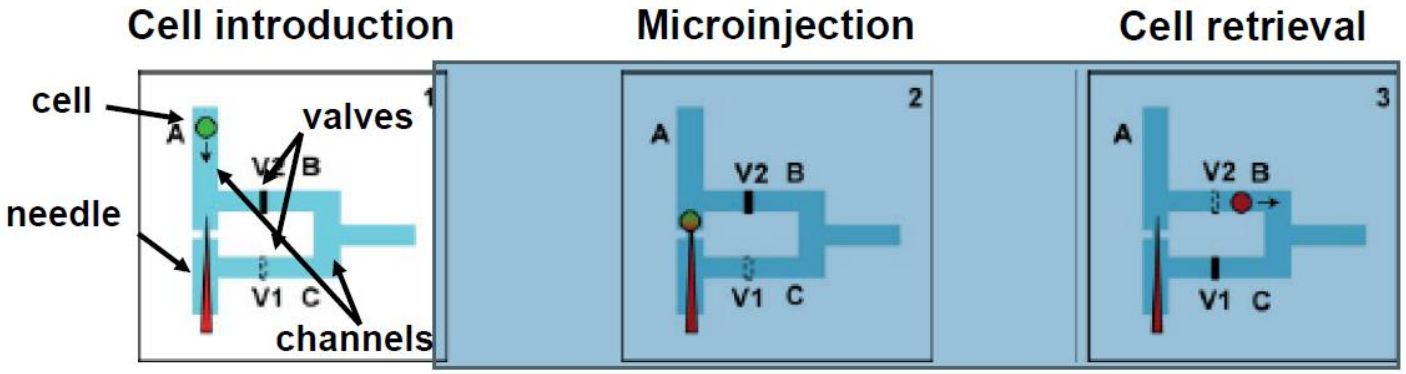

Whole injection process **< 1/10 sec** ⇨ 3600 cells/h

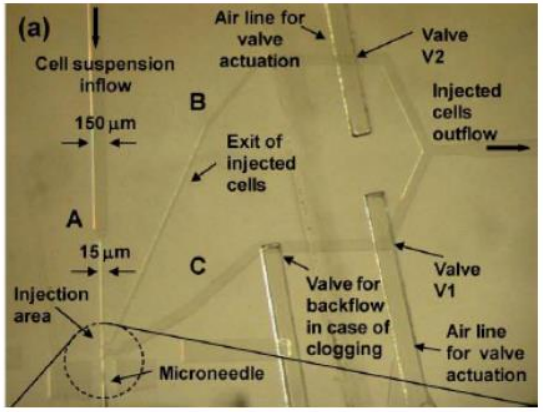

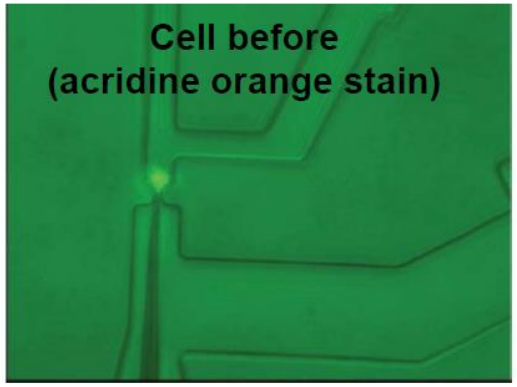

Adamo et al., 2008

Hollow nanoneedles

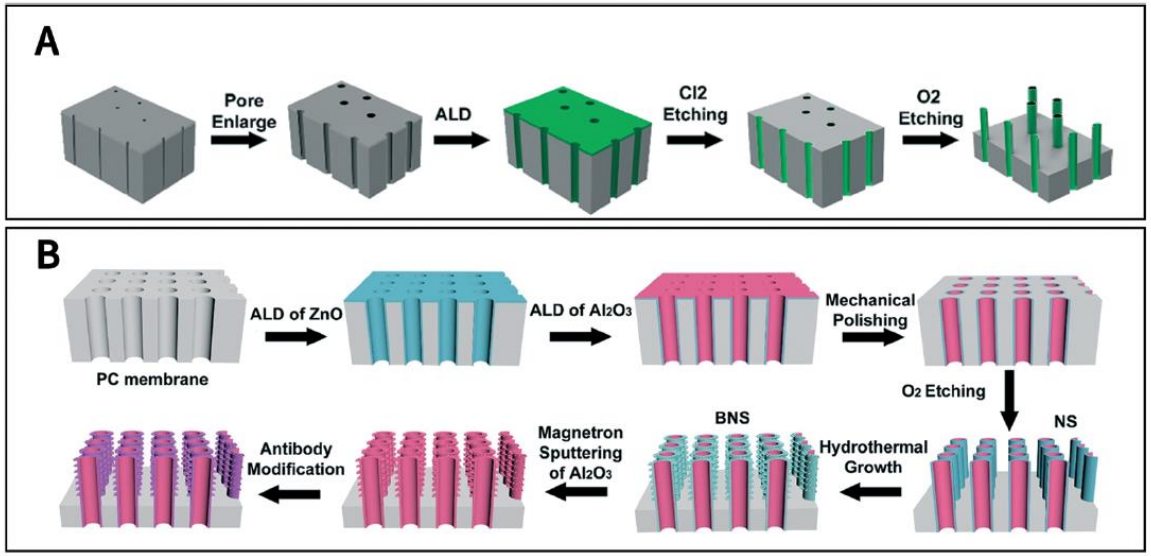

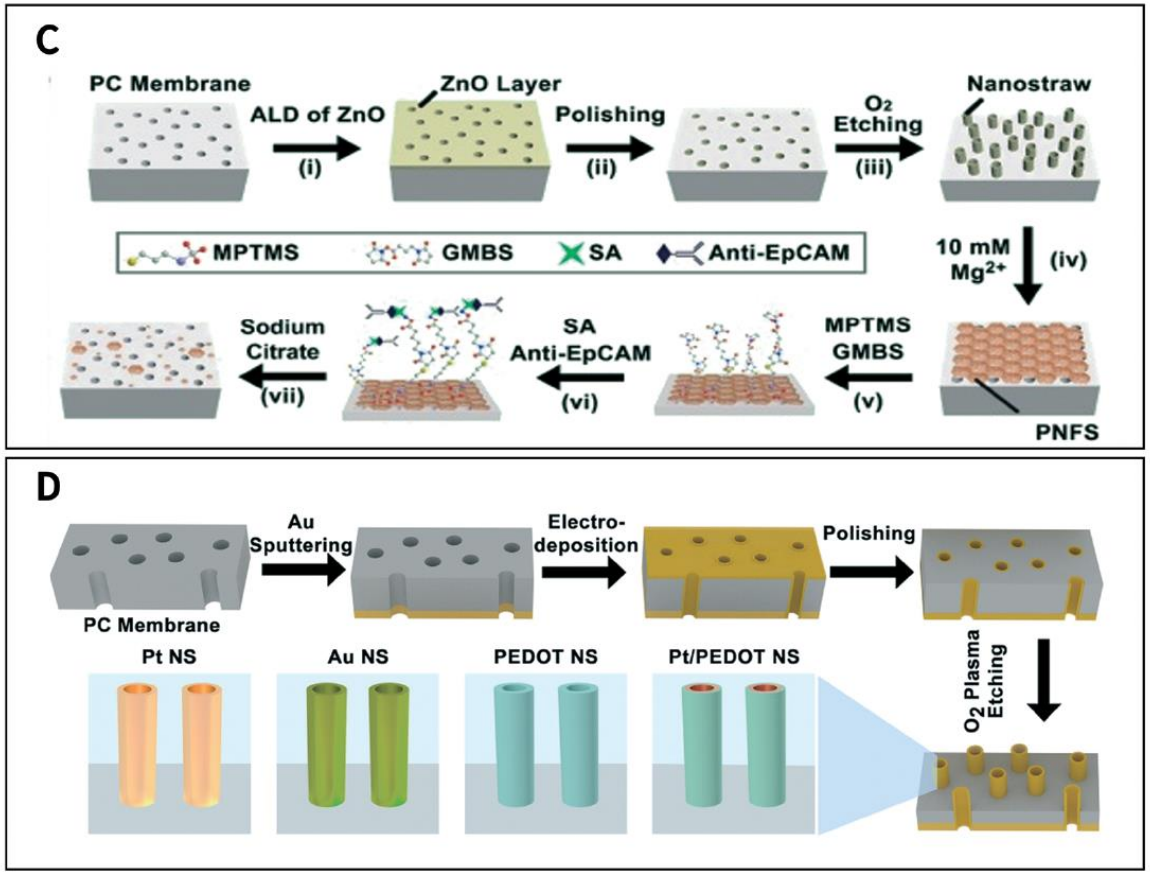

Wang et al, Lab Chip, 2022, 22, 2624–2646

Cell fusion

- Fusion if 2 different cells (or vesicles) to produce a new unit (hybridoma)
- Monoclonal AB production: AB producing cell + cancel cell (immortal cell)
- Fusion adult cell + egg cell
- Fertilization: fusion sperm and oocyte

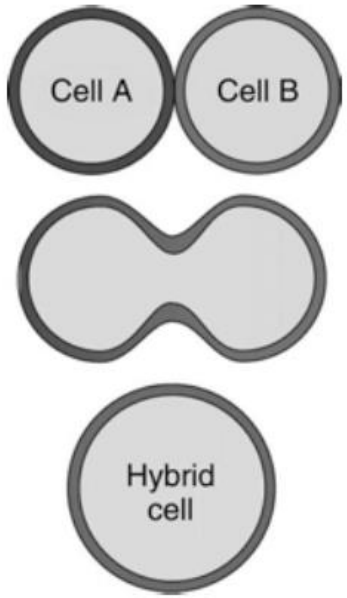

Electrofusion of biological vesicles

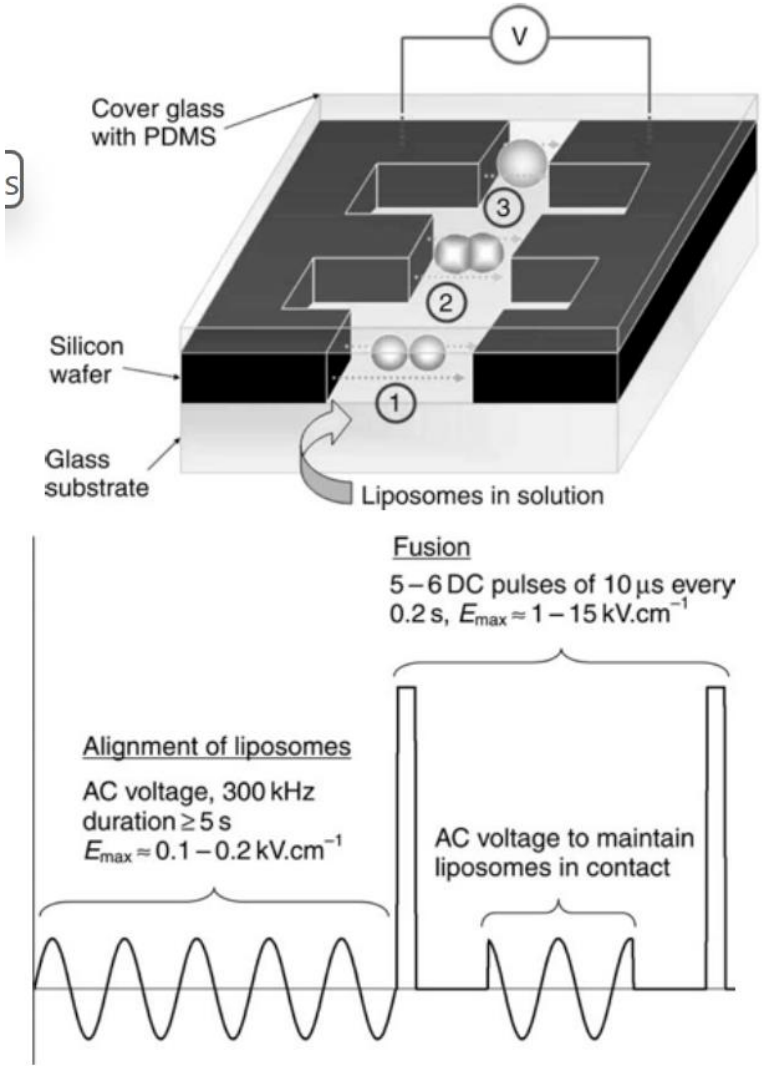

- **AC voltage**: liposome **alignment** between two electrodes
- Short **DC pulse**: **fusion**
- **AC voltage**: maintain **contact** until the fusion is completed

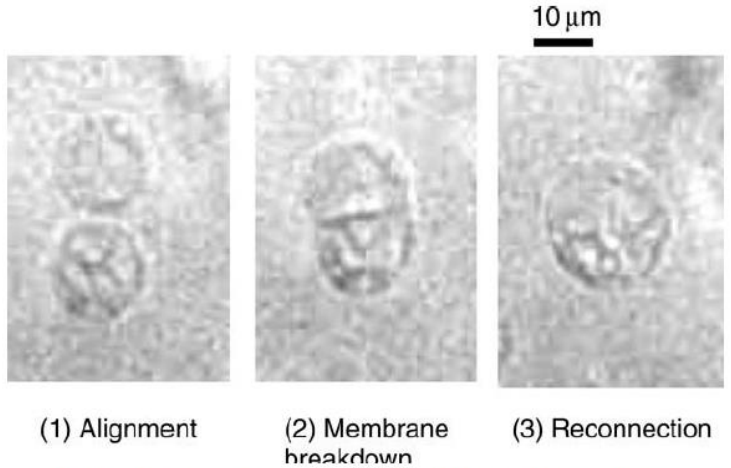

Fusion yield: 75%
Higher yield for larger (>10 µm liposomes)

Tresset et al., 2005

Mechanical phenotyping - Motivation

Correlation between mechanical properties and molecular alterations and diseases

- **Cancer** (change in stiffness linked to the cytoskeleton rearrangement ⇔ metastasis)
- **Malaria** infection (infected RBCs becoming stiffer)
- Cardio-vascular diseases (change in cell membrane stiffness)
- Biomarker for **oocyte/embryo** in ART
  - oocyte quality, oocyte age/maturation, fertilization (increased stiffness), embryo developmental potential, etc.

Promises:
- Label-free measurements
- Non-invasive

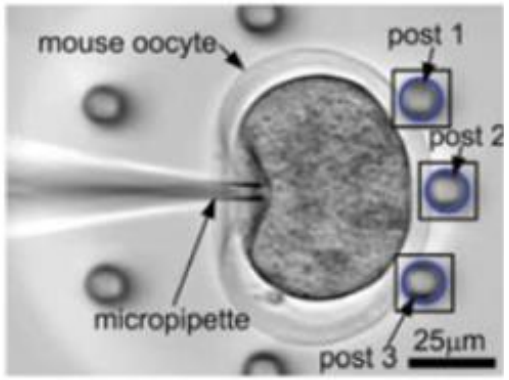

Liu et al., 2012

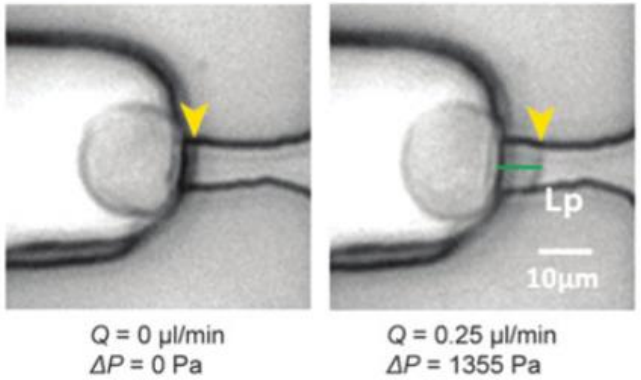

Lee & Liu, 2015

ART: Assisted Reproductive Technologies

Mechanical phenotyping – How?

Conventional approaches

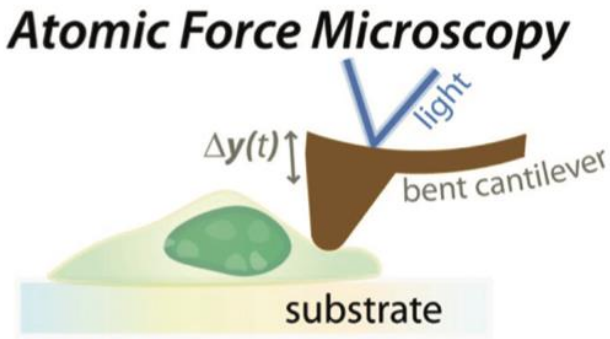

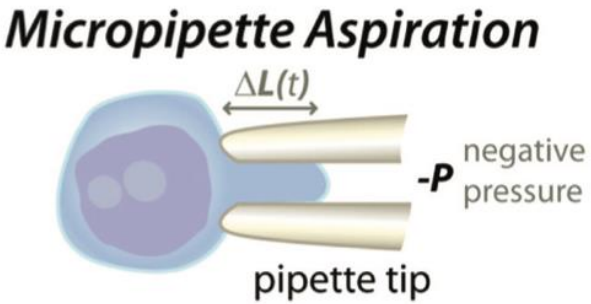

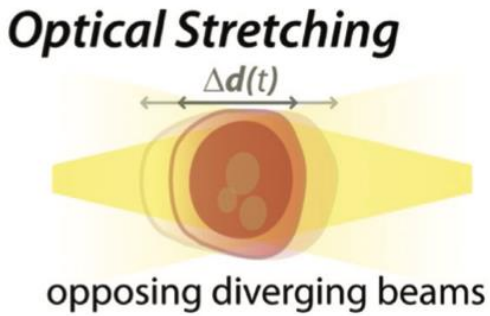

Di Carlo, J. Lab. Autom., 2012

Advantages:

- High-quality/high-content measurements
  - Rheological parameters (*G'* & *G''*)
  - Elasticity (Young modulus, *E*)
  - Viscosity (μ)
- Ideal for small number of cells

Challenges:

- High technicality (trained specialist)
- Low-throughput (one cell at a time)
- No possible automation

⇨ Limited-to-no translational value

For reviews: Hao et al., Biotech. Adv., 2020
Di Carlo, J. Lab. Autom., 2012

Mechanical phenotyping – How?

Microfluidic approaches

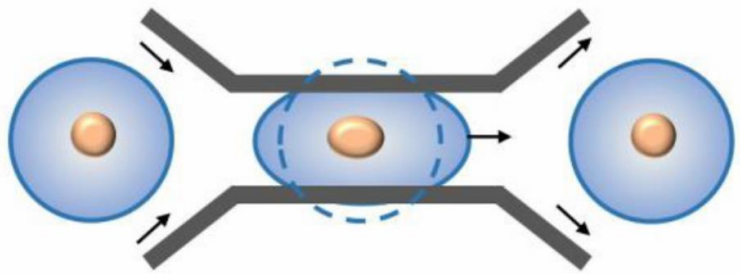

Hao et al., Biotech. Adv., 2020

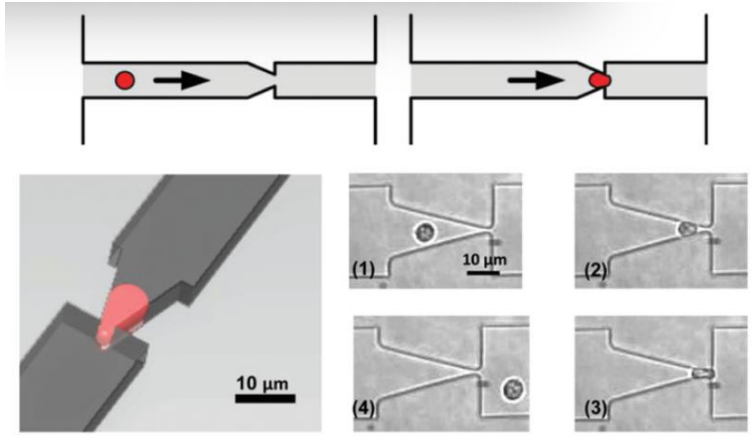

Guo et al., 2012

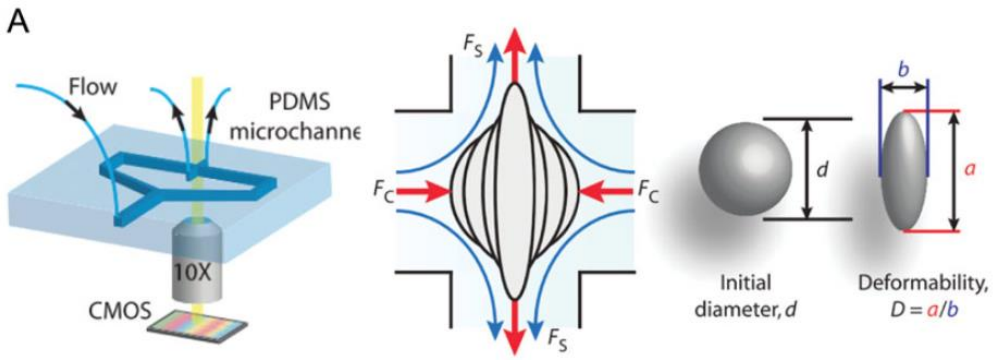

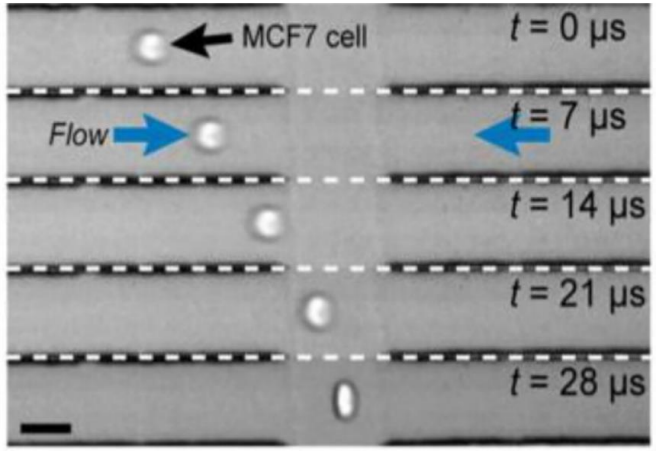

Tse et al., 2013; Gossett et al., 2012

Advantages/Promises:

- Flow-through measurements
- Automation

➪ High-throughput measurements of large populations of cells

Self-propelled particles

❖Self-propulsion: ability of living organisms or synthetic "motors" to move without external drives.

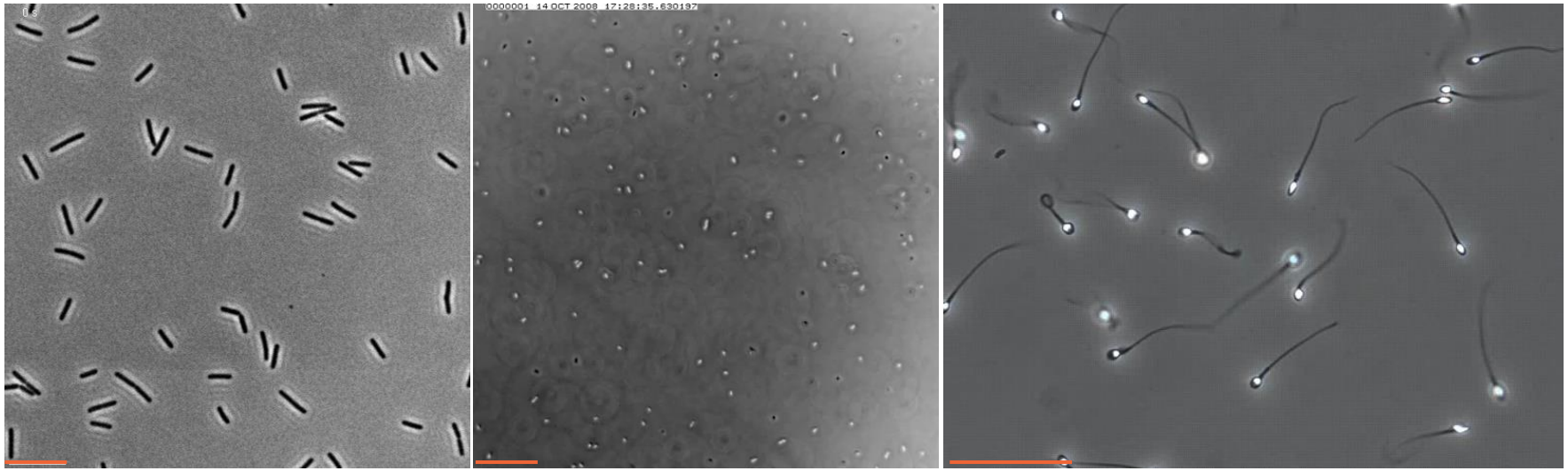

Pseudomonas aeruginosa

Scale bar: 10 µm

Escherichia coli

Scale bar: 10 µm

Sperm cells

Scale bar: 50 µm

(Khanchezar, 2015; Kühn *et al.*, 2021; Tomlinson, 2022)

Context self-propelled particles

- Infertility affects approximately 8 to 12% of couples worldwide
- 40 to 50% of infertility cases are caused by male factor infertility
- Reduced sperm motility

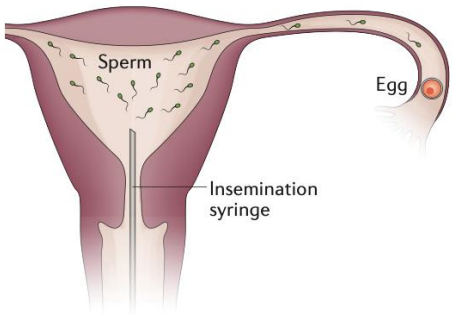

Intra-uterine insemination (IUI)

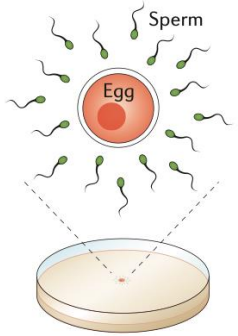

In vitro fertilisation (IVF)

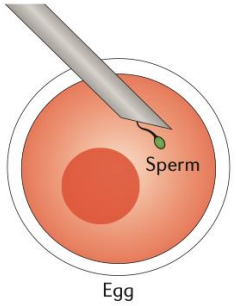

Intracytoplasmic sperm injection (ICSI)

Developed by Gianpiero Palermo at the Vrije Universiteit Brussel in '87

(Nosrati *et al.*, 2017; Chakraborty & Saha, 2022)

Artificial self propelled particles

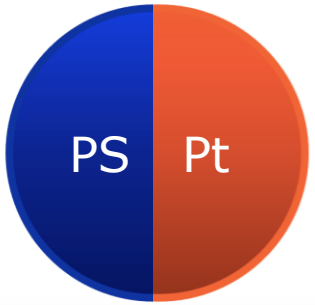

$$2\,H_2O_2 \rightarrow 2\,H_2O + O_2$$

(Self-chemophoresis)

Janus particles: polystyrene beads with one hemisphere coated with platinum catalyst

- **Experimental conditions and parameters**:
- Active particles: 4 μm Janus particles (PS particles covered by Pt, HZDR Dresden)
- Passive particles: 5 μm PS particles
- H_2O_2: 10%
- Microfluidic channel: 375 μm width, three inlets (2 for H_2O_2, 1 for the sample in H_2O)
- Acoustic excitation frequency: 1.9 MHz
- Acoustic excitation power (voltage): varying from P = 0 to 40 mV (300 x amplified)

Acoustic handling – Janus Particles

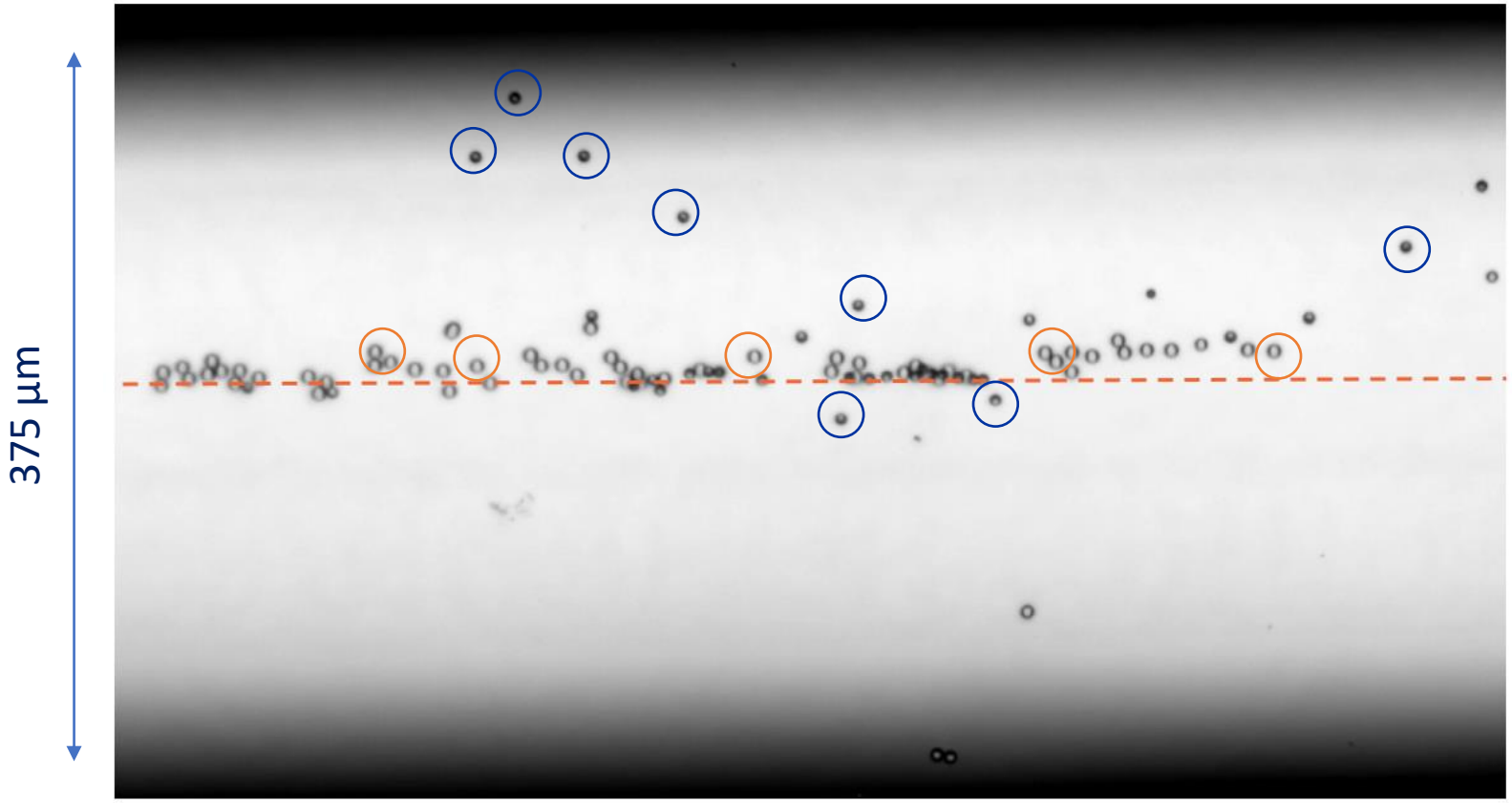

Process conditions:

Frequency: 1.97 MHz

Voltage: 20 mV (amplified by 100)

: Janus particle

: Polystyrene particle

Janus particles in acoustofluidic setup

40 mV (300x)

All particles focused

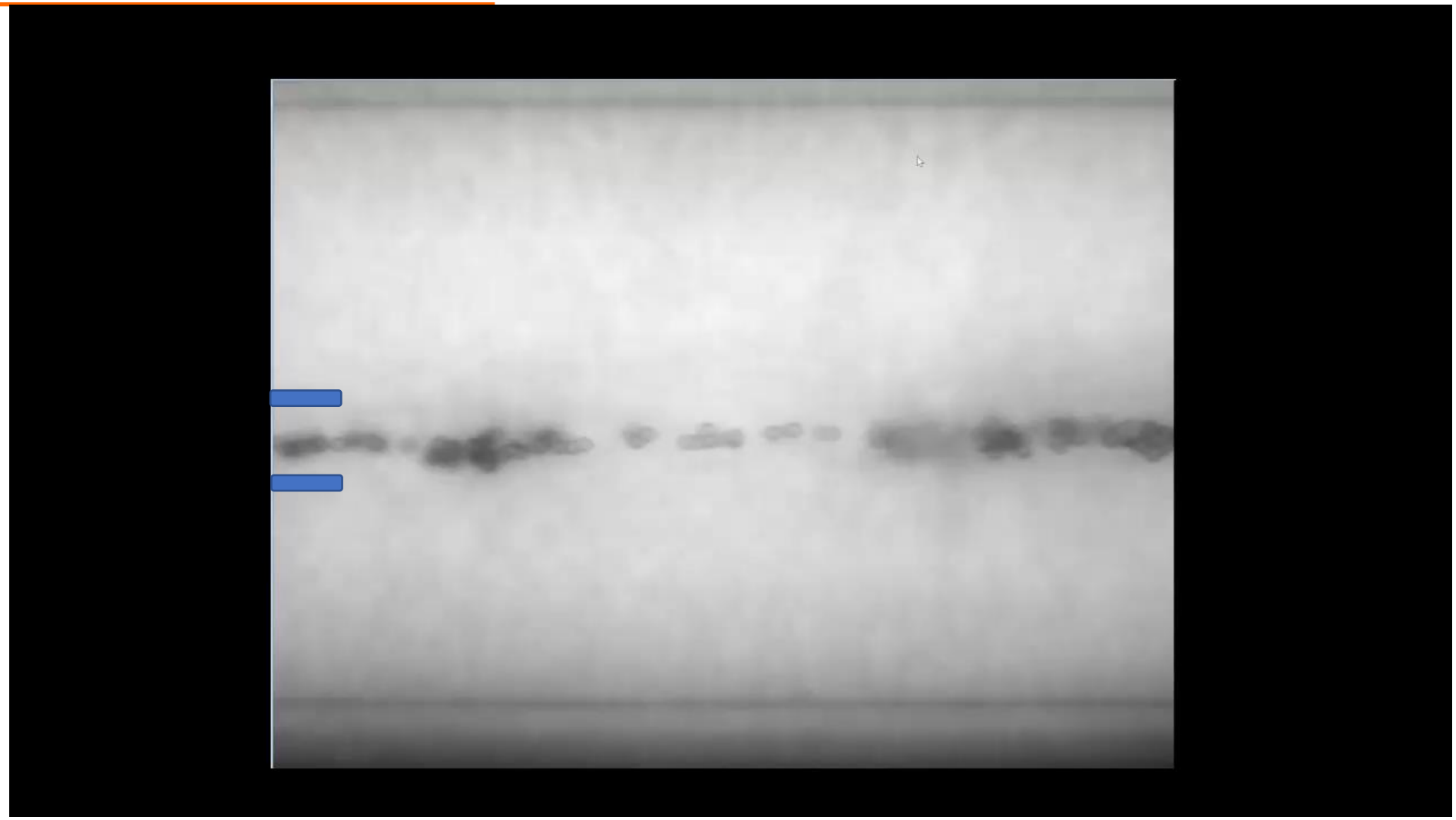

Janus particles in acoustofluidic setup

12 mV (300x)
Escape of
active particles

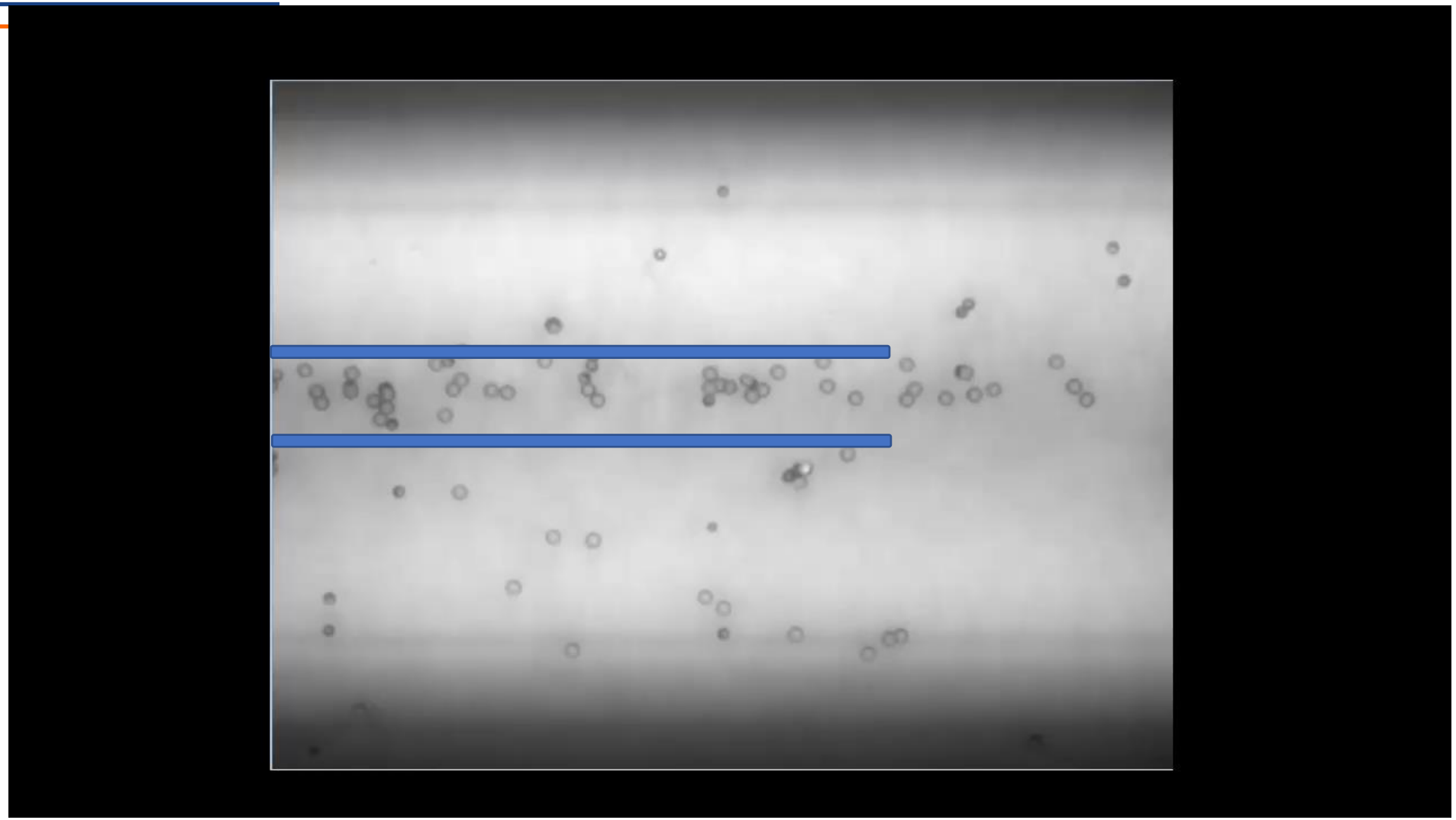

Separation of active particles on motility

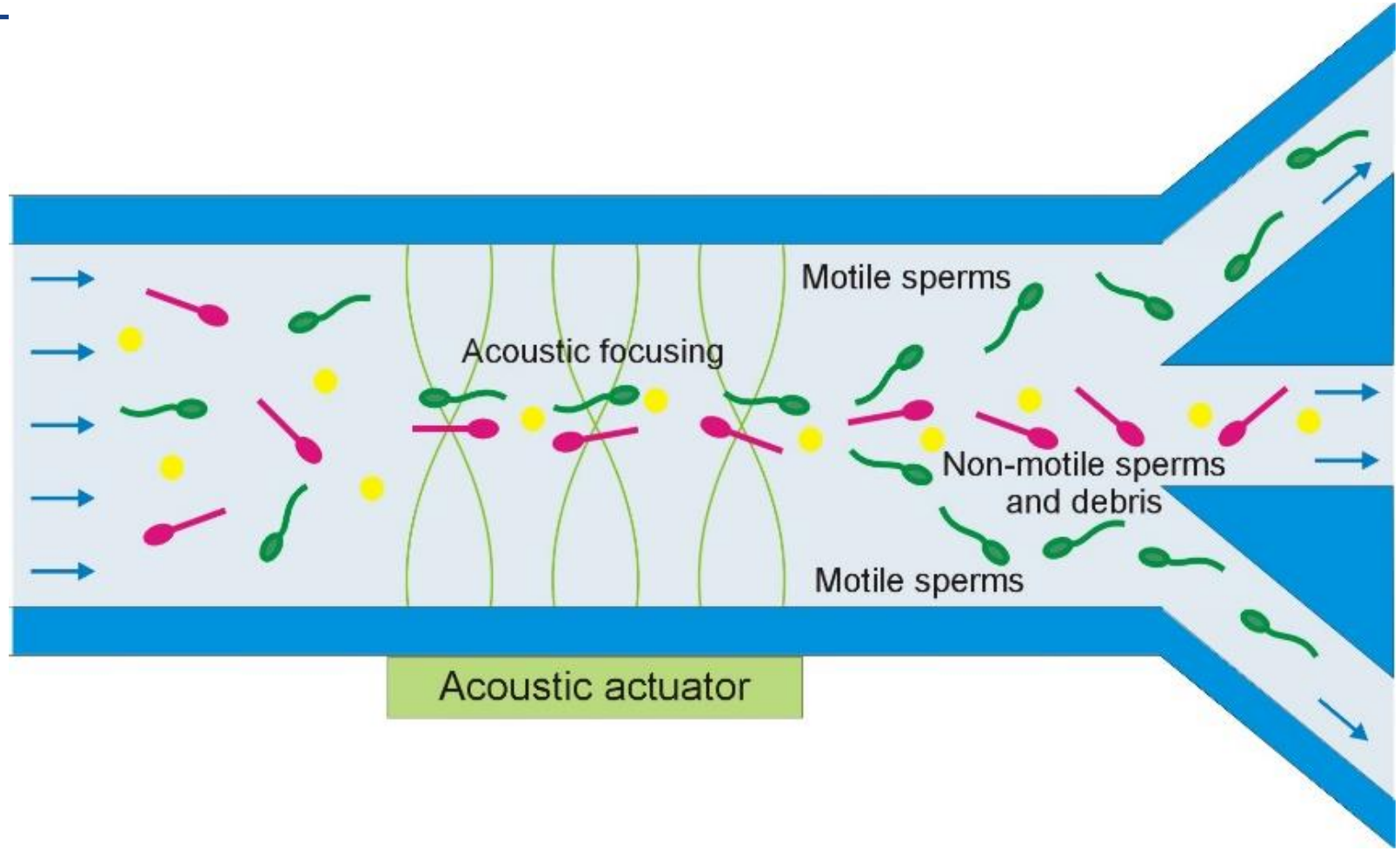

V. R. Misko, L. Baraban, D. Makarov, T. Huang, P. Gelin, I. Mateizel, K. Wouters, N. De Munck, F. Nori and W. De Malsche, Selecting active matter according to motility in an acoustofluidic setup: self-propelled particles and sperm cells, Soft Matter **19**, 8635 (2023)

Numerical experiment on motility focusing

Escape of motile self-propelled particles from the acoustic focusing potential and their separation from non-motile species: the motile sperms are characterized by high ($v = 2v_{flow}$), moderate ($v = 2v_{flow}$) and zero motility.

The trapping potential is strong enough to focus all the species. Motile and non-motile particles can be separately detected away from the focusing potential, at $x = 15$. Motile swimmers escape the focused flow and can be detected by the side detectors while non-motile particles remain focused.

The trapping potential is reduced to 0.25. The motile particles partially overcome the barrier and thus flow outside the focused flow of non-motile particles. High motility species overcome the barrier easier and can be separated not only from non-motile species but also from less motile species.

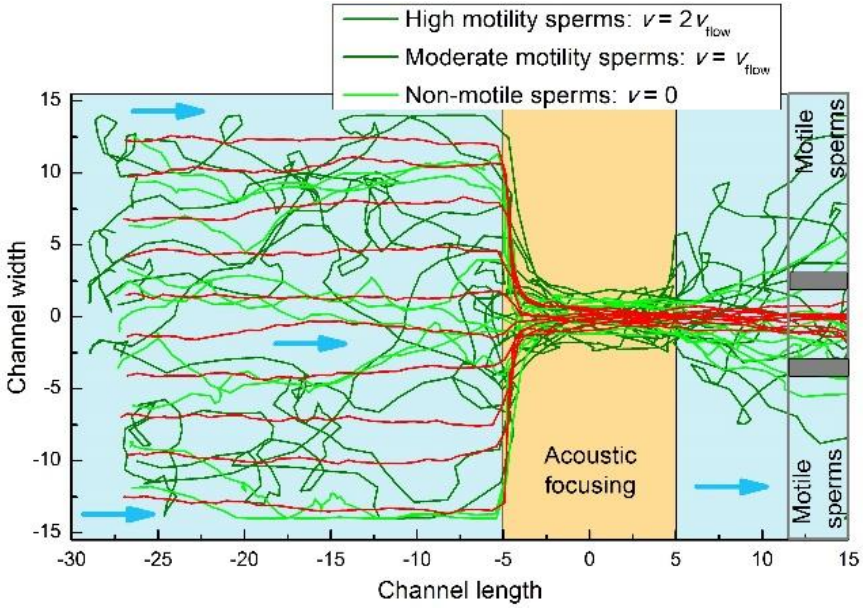

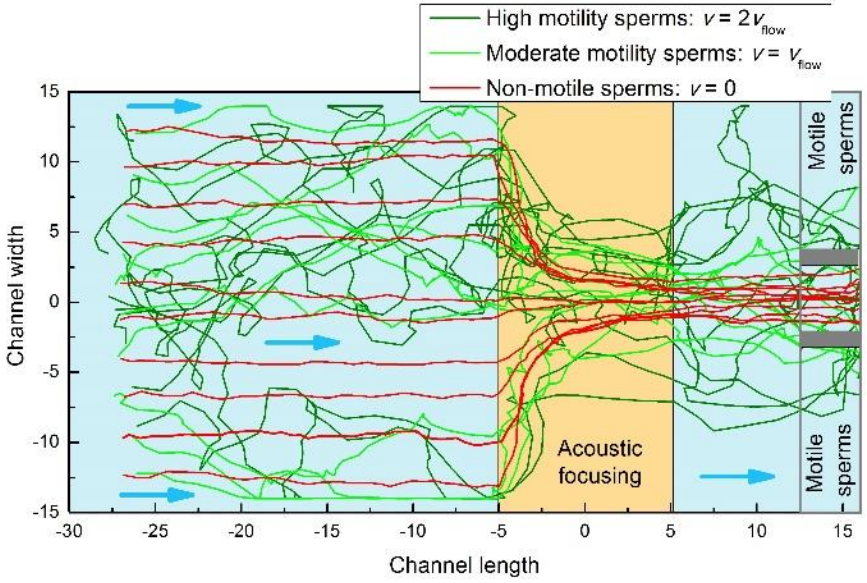

V. R. Misko, L. Baraban, D. Makarov, T. Huang, P. Gelin, I. Mateizel, K. Wouters, N. De Munck, F. Nori and W. De Malsche, Soft Matter **19**, 8635 (2023)

Experiment sperm focusing

- P = 50 mV:
- **Weakly motile/non-motile sperm & debris** are **focused** by the acoustic potential
- **Highly motile sperms escape** the focusing potential (selection) and can be **collected separately** (separation)

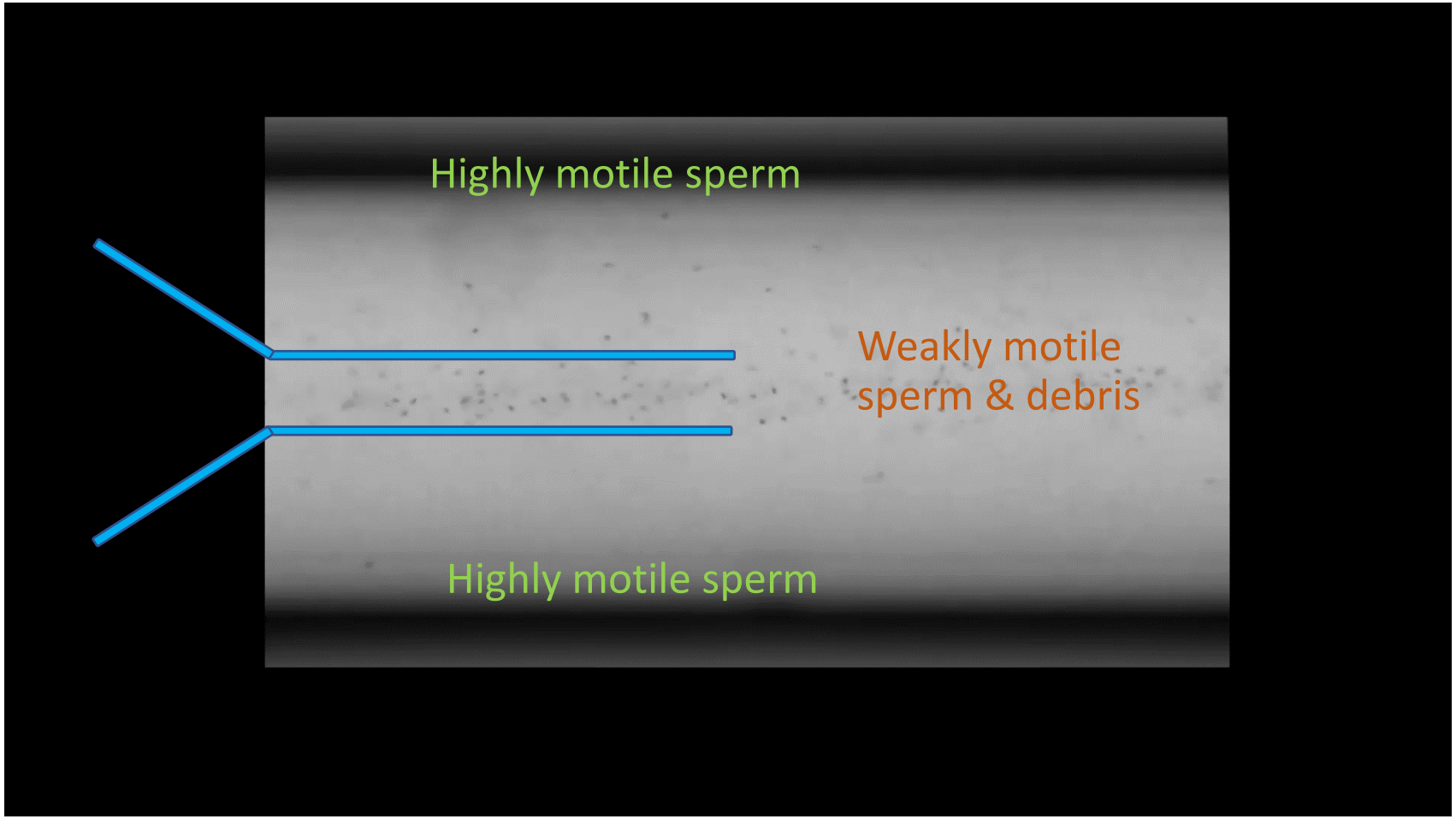

Acoustic selection most motile sperm cells

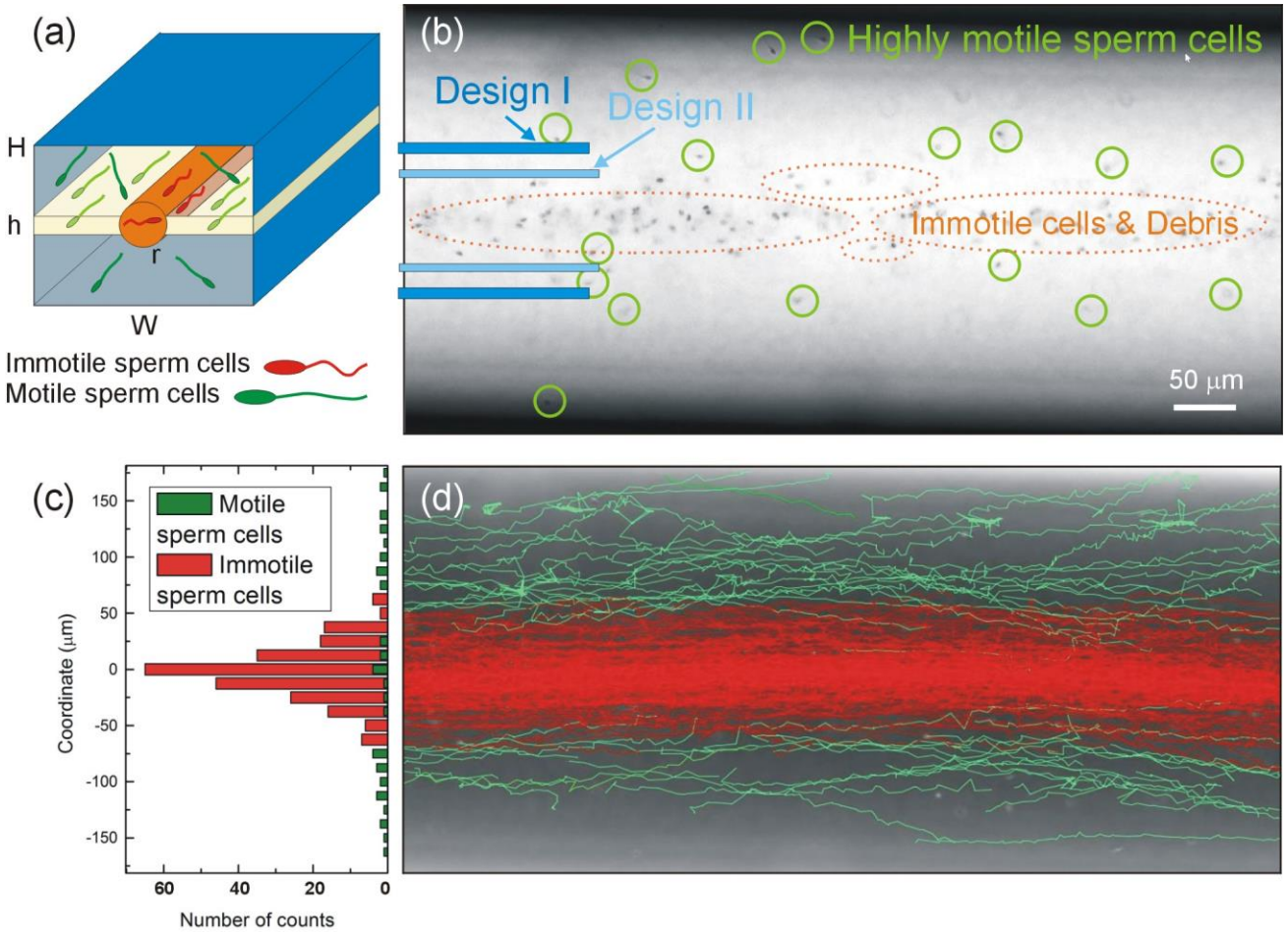

V. R. Misko, L. Baraban, D. Makarov, T. Huang, P. Gelin, I. Mateizel, K. Wouters, N. De Munck, F. Nori and W. De Malsche, Soft Matter **19**, 8635 (2023)

Trapping of sperm cells

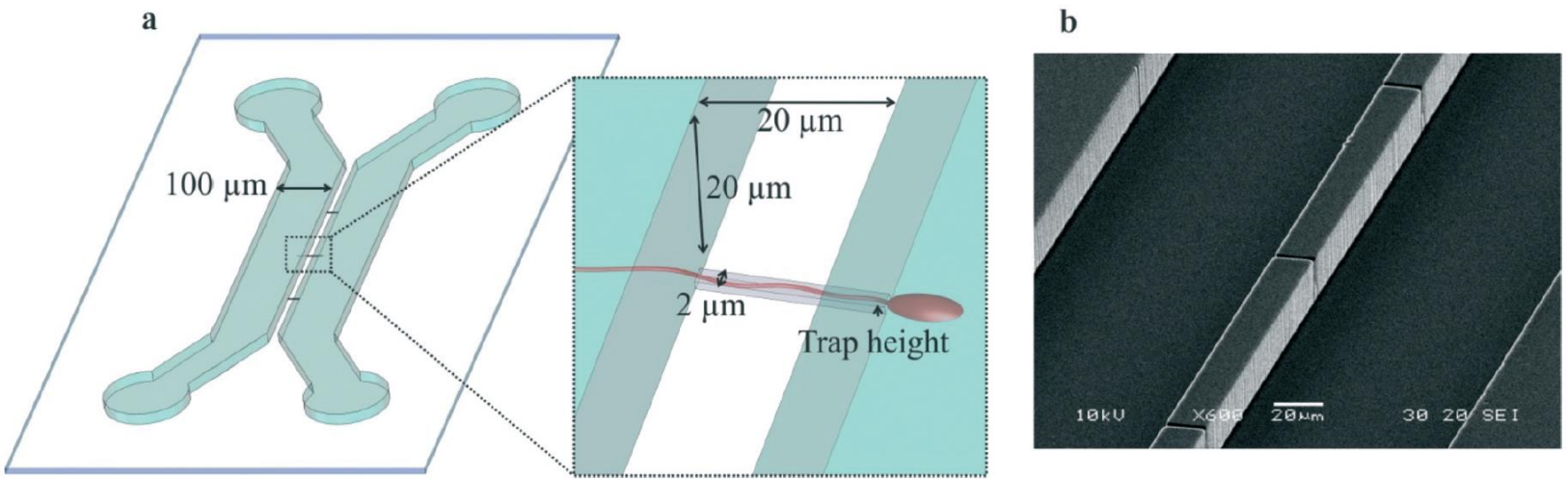

Fig. 1 Illustration and imaging of the microfluidic platform. The PDMS chip design, when bonded to a glass substrate (a), consists of two main channels (width 100 µm, height 20 µm) and twenty side channels (width 2 µm, length 20 µm), which connect the main channels. The height of these side channels, *i.e.* trap height, is 1, 1.5 or 2 µm. The topography of the PDMS device (1 µm high side channels facing upwards) was studied using SEM (b).

de Wagenaar et al., Lab Chip,2015, 15,1294–1301

Single sperm cell analysis

The acrosome reaction, which involves the **activation of proteolytic enzymes to digest the zona pellucida, plays a crucial role in the fertilizing potential of spermatozoa**.

In vitro analysis using the ionophore-induced acrosome reaction (ARIC) test was shown to be effective in predicting fertilization potential in IUI and IVF treatments.

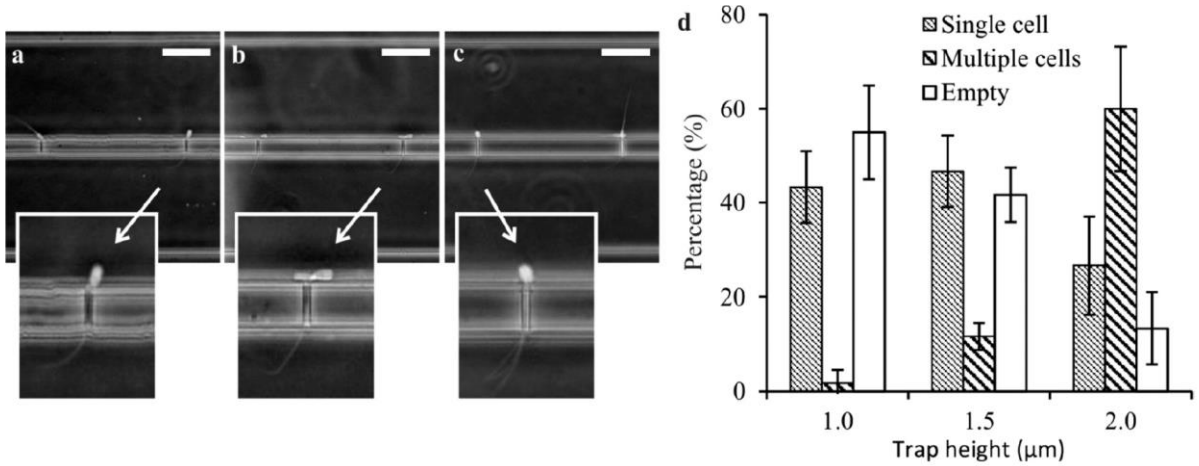

Fig. 3 Entrapment of sperm cells in 2 μm wide PDMS traps with a height of 1 μm (a), 1.5 μm (b) and 2 μm (c). Sperm cells were entrapped in a head-first or tail-first orientation. The percentage of traps filled with no cells, a single cell or multiple cells was recorded and plotted *versus* trap height (d). The percentage of single cell trapping was highest for chips with a trapping height of 1.5 μm. The highest ratio of single *versus* multiple cell trapping was obtained using chips with a trap height of 1 μm. Increasing the trap height resulted in an increase in multiple cell trapping and a decrease in the amount of empty traps (experiments per trap height n = 3, all scale bars 50 μm).

Damaged or reacted Acrosomes (FITC-PSA)

Intact acrosomes (LysoTracker blue)

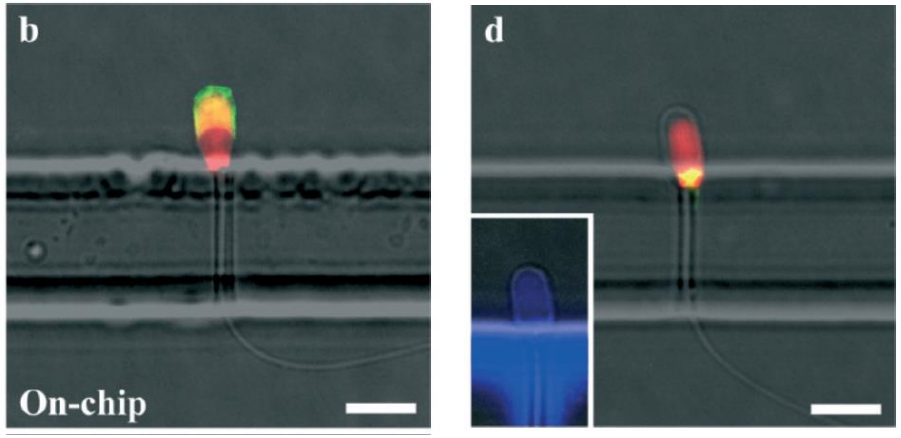

Conclusion

- Separation/detection methods available compatible with single cell content
- Major challenge dilution and sample preparation
- Cell lysis methods available, changes during lysis likely impactful
- Well-developed electroporation methods available
- Tools available for handling and mechanically characterizing cells
- Identification (and hence separation) of compounds key for comprehensive analysis
- Main challenge: no modification of analyzed species during analysis and sample prep